Interactive comment on “Early season mesopelagic carbon remineralization and transfer efficiency in the naturally iron-fertilized Kerguelen area” by S. H. M. Jacquet et al.

Biogeosciences Discuss., 11, C3944–C3947, 2014

C. Jeandel (Referee #2) catherine.jeandel@legos.obs-mip.fr
Received and published: 30 July 2014

Dr Jacquet and co-workers report an interesting study variability of the mesopelagic barite in excess along a broad N-S transect in the Kerguelen area, from which they deduce the zonal variability of the POC export. They also performed this study within a meander east of the Kerguelen plateau, transect allowing them to follow the temporal evolution of these oceanic parameters. They eventually compare some of their results (when possible) to earlier data obtained at the same location but at fall, which provides an insight on the seasonal variability of the Baxs distribution, POC export (EP) and their remineralization rate estimate, that they compare to primary production (PP and EP being published in companion papers of the same issue). The set of data is of good quality, the complexity of the area made the interpretation challenging, difficulty which is honorably overcame by the authors. This work deserves to be published in Biogeosciences, but not without some improvements proposed below.

General Comments

Reviewer: The whole paper is based on the use of Baxs as proxy of the POC remineralization, proxy that was well described by many preceding works of the same authors and oth- ers. Indeed, the Baxs mesopelagic maxima is ubiquist; Bishop, Dehairs and others demonstrated that micro-crystals of barite precipitates in biological microenvironments (fecal pellets, aggregates. . .) , and that the release of these micro-crystals yielding the observed maximum corresponds to the disintegration of this biological material, con- comitant to the maximum consumption of oxygen, the latter being related to POC oxi- dation. However, this reasoning and the empirical relationship allowing relating Baxs to POC remineralization is based on one dimensional approach. The Kerguelen plateau is particularly dynamic, and several preceding works discuss (and even propose a modelling, for the Pa/Th distribution, Venchiarutti et al, 2008) the importance of the advection on the fate of Trace Elements and isotopes on the plateau and around. I am concerned by the fact that the impact of advection and internal tides is never dis- cussed in this work. For example, the maximum of Baxs at the reference station is considered only as a remnant signal from a preceding bloom, occurring in late winter. Other works are observing maxima of LSi, particulate Fe, Mn and Al (van de Merwe, Lasbleiz et al) that could be advected from the Leclaire Rise, located 75 km north west of R-2. . .knowing that re- suspended sediments are also enriched in Baxs (as shown in this work at stations A3 for ex) why is the hypothesis of such horizontal transport not discussed here? On the plateau, what is the importance of horizontal versus vertical transport? This should be more deeply considered in the present manuscript.

Reply:
First, to estimate POC remineralization rates we used an algorithm relating Baxs contents to the rate of oxygen consumption that was deduced via a 1-D advection diffusion model applied on highly resolved, precises dissolved O2 profiles along 6°W in the Southern Ocean (Shopova et al., 1995, Dehairs et al., 1997). During the KEOPS 1 cruise, by comparing mesopelagic oxygen consumption rate obtained using the Winkler method and this obtain using Baxs contents and the above-mentioned algorithm, the correlation was significative (R^2=0,90, $p<0.05$). We concluded in the validity of the algorithm in the Kerguelen area. This correlation and discussion about oxygen consumption rate have been added in the ms.
Then, Baxs peak at the K2 reference station is surprising in that in “ HNLC / no bloom / low productivity / low export” conditions we observe a signal that we attributed to a previous/ winter production and export event. Nitrate contents and isotopic enrichment also relate an imprint of winter uptake (Dehairs et al., this issue), and low Si:C and Si:N ratios potentially reflect a previous diatoms development (Lableiz et al., this issue), which is consistent with high dissolution rates of BSi in surface (Closset et al., this issue). Both results suggest the occurrence of a winter production and

remineralization event. In Bowie et al., Quéroué et al. and van der Merve et al., (both this issue), authors report that lateral transport of lithogenic matter from the Leclaire Rise (a large seamount located west of station R) would explain local maximum at 500 m depth and deeper, in particulate and dissolved trace metals. This is also corroborated in Lasbleiz et al. (this issue) with LSi data exhibiting a maximum at R station at 500m reflecting particulate lithogenic input. However, the Baxs maximum at K2 is relatively shallower (maximum at 300 m). Also, the size fractions of particles above and below 500 m depths are different at this station. We don't think that the upper 500 m Baxs signal (and maximum at 300 m) could be related to major Ba advection. We can however not exclude the impact of advection on the whole Baxs profile, even if salient Ba peak are not present deeper 500 m. Also, the Baxs was calculated as the difference between total Ba and lithogenic Ba using Al as the lithogenic reference element. During KEOPS2, at most of sites and depths the biogenic Baxs represented >95% of total Ba. At K2, the lithogenic Ba reached up to 20% solely in the upper 80 m.
Concerning station A3 on the Plateau, the lithogenic contribution is relatively important, mainly below 400 m where we observe important Ba and Al peaks. Particles size spectra clearly indicated at A3 sediment resuspension. We mentioned in the ms. that for profiles at station on the plateau, bottom waters with evidence of lithogenic input were not taken into account when calculation DWAv Baxs values. As also reported for station R-2, the lithogenic part at A3 on the Ba signal was minor (expect near the bottom due to sediment resuspension). Concerning the importance of lateral advection on the plateau in setting the Baxs signal, we added a discussion in the ms. (we referred to the work of Venchiarutti et al., 2008 and to Baxs profiles obtained on the plateau during KEOPS 1).

Sentences have been added in paragraphs first mentioned to as 4.1 and 4.2. These paragraphs moved to the results section.

Detailed comments

Reviewer: In the abstract, it should be explicitly written that the “mesopelagic POC remineralisa- tion” reported here is deduced from Baxs proxy: this would be more precise
Reply: Done

Reviewer: -In the introduction and section 3.2, no reference is made to E. Sternberg work, who also demonstrated (with F Morel) that Baxs in the surface water is “scavenged Ba” but not immediately crystallized as barite, and brought some clues on the seasonal “rhythm” of the barite formation by studying a “short time series” in the Mediterranean Sea. This could be added.
Reply: Three references related to the works of E. Sternberg (2005, 2007 and 2008) have been added in the introduction and in section 3.1.

Reviewer:-At the end of the introduction, I found question 1) not clearly written, please explicit better what was this first motivation.
Reply: Question has been reformulated, and explanations have been added in the introduction and section 2.1.

Reviewer:-Sampling and analyses: neither the blanks, nor the reproducibility are given, should be added.
Reply: Details have been added in section 2.2.

Reviewer:--In the result section, the surface maxima observed at E1 and the pic at 100 m at E4-E are not described. Could be done.
Reply: The surface Baxs signal at E1 and E4 has been described (paragraph 3.1)

Reviewer:-Paragraph 4.1: the first sentence is not clear as it is written: the link between “low productivity, low export and highest DWAV is not direct, which appears to be the case at the first reading of the sentence: rephrase.
Reply: the sentence has been revised.

Reviewer:- End of the same paragraph: about the hypothesis of "recurrent winter production" that might explain the R-2 maximum. . .was such phenomena visible and already observed with the satellites?
Reply: We checked Chla satellite image from the Giovani online Visualization and Analysis system (NASA GES DISC). It appears that for different years, the R-2 and KERFIX area could indeed be subject to enhanced productivity during early spring periods, but it is not salient for winter period. The sentence has been revised in the ms.

Reviewer:- Discussion, station in the meander (4.3): I appreciated the evolution of the different ratios considered here, that allows following an interesting temporal evolution of the biogeochemical dynamic in this "recirculation". Fig 5b and the related discussion would be easier to follow if the authors could add an inset to the Fig3, inset showing the full depth profile of Baxs at the stations TNS-6 and E-1 where bathypelagic processes are suspected.
Reply: Fig3h has been added showing the full depth profile of Baxs at TNS6 and E-1 vs. E4-E. Fig3h is referred in the ms in section 3.1 and 4.2.3.

Reviewer:-Table 1: in the date of sampling, the precision "2011" is perhaps not useful
Reply: "2011" has been removed from the dates of sampling.

Reviewer:--Figures: None of the figure proposes a circulation scheme, that could be helpful (in connection with my general comment)
Reply: The two branches of the Fawn trough Current have been added in Fig1a. Sentences have been added in section 2.1.

Reviewer:-In the caption of fig 4: the authors could add "POC, deduced from the Baxs maxima"
Reply: Done

Interactive comment on "Early season mesopelagic carbon remineralization and transfer efficiency in the naturally iron-fertilized Kerguelen area" by S. H. M. Jacquet et al.

Anonymous Referee #1
Received and published: 4 July 2014

Review of Early season mesopelagic carbon remineralization and transfer efficiency in the naturally iron-fertilized Kerguelen area by Jacquet et al.

Overview and major comments

This study is part of the KEOPS2 special issue investigating the downward flux of car- bon in a naturally iron fertilized bloom in the southern ocean (Kerguelen). Although we recently gained knowledge on how POC is exported out of the sunlit layer of the ocean following natural fertilizations (Blain et al., 2007;Chever et al., 2010;Morris and Charette, 2013;Pollard et al., 2009;Le Moigne et al., 2014), a major unknown remains about the fate of the particulate organic carbon further down in the water column. This process is critical to understand if one wants to assess the genuine effect of Fe fertil- ization of atmospheric CO2 concentrations. Jacquet et al present mesopelagic carbon remineralization rate data in the vicinity of the Kerguelen Islands. The paper focuses primarily on the differences in carbon remineralization rate between high and low iron regions and at different stage of the bloom evolution with emphasis on the efficiency with which POC is transferred into the ocean's interior. While I am not an expert in the "Barium" technique, my feeling is that the methods employed to derive estimates car- bon remineralisation rate are well developed and sound, as are the estimates of POC export and primary production estimates presented elsewhere. Nevertheless, before I can recommend the manuscript for publication, significant mod- ifications and improvement are necessary. The discussion lacks substance and only focuses on a basic description on the differences between difference sites sampled and the KEOPS1 results.

Reviewer: The authors do not clearly assess to which extent their metrics (r ratio, T400/800) are impacted by the integration time of the various technique they used. The PP, the Th- POC export and the Baxs C remineralisation rate are all express as daily rates (g C m-2d-1). However, PP (likely from bottle incubation, although the information is not available to the reader yet as Cavagna et al is not published) is integrated over a day (24or 12 hours incubation I assume) while the Th-POC export over a month (Le Moigne et al., 2013;Henson et al., 2011). The Baxs integration time seems less constrained and may well be over that of the Th-POC export. To overcome that problem, (Henson et al., 2011) integrated PP over a month which is comparable with the time-period which the Th technique integrates the POC-fluxes over. For instance, this has relevance to explain why the largest remineralisation rates (and subsequent r ratios, and Ts) are observed in the HNLC zone and why Ts (400 or 800) are on occasions larger than 100%. This needs to be assessed and discussed.
Reply: As detailed further below this has been discussed and revised in the ms.

Reviewer: Also, the manuscript would benefit of integrating recent observations about the mech- anisms responsible driving the transfer efficiency in high latitude with highlights from some of the paper listed below (non exhaustive list though)(Henson et al., 2012;Le Moigne et al., 2012;Lam et al., 2011;Lam and Bishop, 2007;Maiti et al., 2013;Wilson et al., 2012;Buesseler et al., 2007;Morris and Sanders, 2012) etc... These propos dif- ferent processes as potential mechanisms to explain patterns in POC export/transfer efficiency in high latitude. It would be valuable to examine and discuss the dataset presented here regarding how the various locals Fe supply observed around the Ker- guelen Islands impact patterns in POC export/transfer efficiency in high latitude. I do understand that this paper is part of a special issue and that a more comprehensive overview paper including this dataset might be put together later on. Nonetheless, a more thorough discussion of the results and their implications would be welcome to meet the publication criteria defined by Biogeosciences.
Reply: Discussion and references have been added in the ms.

Reviewer: Finally, the manuscript would benefit from serious improvement regarding language. It needs to be very thoroughly revised by a native english speaker, the text (including references list) is currently littered with typos and awkward sentences which makes the paper hard to read and sometimes confusing.
Reply: Language has been revised

Reviewer: Also, some manuscripts referenced in the text do not appear in the references list and the acronyms are not consistently used throughout the text.
Reply: References will be revised

Minor comments

*P4*_P9038, L10: Please refer to (Le Moigne et al., 2014) for most recent advance on the topic
Reply: the reference has been added in the text.

*P4*_P9038, L21: "and, and, and" rephrase. See general comment about language
Reply: the sentence has been rephrased.

*P5*_PP9039, L13: Any feeling on how long the Baxs technique intergrates the C remineralisation rate for?
Reply: The time window integration of the Ba signal ranges from few (1-3) days to few (1-2) weeks.

*P5*_P9039, L25: references
Reply: done

*P6*_P9040, L19: Dates please
Reply: dates have been added in the text

*P9*_P9043, L10: please specify "rates" after remineralization.
Reply: done

*P11*_P9045, L9: What are you referring to?
Reply: We referred to section 3.1. Note that these sentences have been rephrased as requested by the second reviewer. Some sentences about the surface Baxs signal have been added in section 3.1.

*P11*_P9045, L15: Four or for? needs rephrasing
Reply: we rephrased

*P11*_P9045, L28: The two
Reply: done

*P12*_P9046, L20 : Include (Robinson et al., 2014)
Reply: done

*P13*_P9047; L6: Sequestration efficiency refers to the sequestration efficiency (the excess of POC export divided by the excess of DFe supply) as defined in (Blain et al., 2007) and re-used in (Pollard et al., 2009;Morris and Charette, 2013;Chever et al., 2010;Le Moigne et al., 2014). Please stick to the established terminology to avoid confusion.
Reply: done

*P13*_P9047, L8: untill !!!! ("up to" would be adequate here).
Reply: done

*P13*_P9047, L10 and Table 2: EP/PP is called export efficiency (Buesseler, 1998)

Reply: OK we mentioned it.

*P13*_P9047, L14: You imply here that remineralisation rates are a function of PP and export here (low PP/export; high remineralisation). Why C remineralisation rates would be negatively correlated with PP and export in the HNLC region?
Reply: The negative relationship between PP and PP and differences in EP/PP vs. MR have been discussed. The main reasons to explain the differences are the time delay between signals and differences in diatoms and sinking material.

*P13*_P9047, L16: Could you specify sampling depth? Trull et al and Laurenceau et al are not available yet.
Reply: done

*P13*_P9047, L22: Please provide information or references on what mechanism could potentially lead to an important winter production and subsequent export, *P13*_P9047, L27: you mean a previous winter bloom? and *P14*_P9048, L3, Is November in the Southern hemi- sphere wintertime? I believe not. The argument (or the date indicated) is not valid. Comparing that to previous estimation of C remineralization rate (from Baxs and other technique) estimated in other HNLC regions (and perhaps a bit further in the season) would provide valuable information on whether the HNLC region has intrinsically a more active heterotrophic community early in the season or whether the high C remineralisation rate observed here are a artefact of the Baxs technique integration time.
Reply (P13_P9047, L22, P13_P9047, L27 P14_P9048, L3): We checked Chla satellite image from the Giovani online Visualization and Analysis system (NASA GES DISC). It appears that for different years, the R-2 and KERFIX area could indeed be subject to enhanced productivity during early spring periods, but it is not salient for winter period. The sentence has been revised in the ms. Also, as reported above the integration time of Ba ranges from several days to week and we can exclude a potential artefact of the Ba technique. According to results from Christaki et al. (this issue), the prokaryotic activity at station R-2 was low but column-integrated bacterial production (BP) below 150 m represents 41% of the 900 m column-integrated value, indicating that important mineralization of material transferred from the surface occurs at mesopelagic depths. Other parameters also show that an export event occurs at R-2 (Lasbleiz et al., this issue- Si:C, Laurenceau et al., this issue- particle composition, Dehairs et al., this issue- nitrate isotopes). Discussion has been revised.

*P18*_P9052: Nothing about the large remineralisation rate at the reference HNLC site in the conclusion?
Reply: Conclusion has been revised.

Early season mesopelagic carbon remineralization and transfer efficiency in the naturally iron-fertilized Kerguelen area

Jacquet S.H.M.[1], F. Dehairs[2], D. Lefèvre[1], A.J. Cavagna[2], F. Planchon[3], U. Christaki[4], L. Monin[5], L. André[5], I. Closset[6] and D. Cardinal[6]

[1]Aix Marseille Université, CNRS/INSU, IRD, Mediterranean Institute of Oceanography (MIO), UM 110, 13288 Marseille, France

[2]Vrije Universiteit Brussel, Analytical, Environmental & Geo-Chemistry and Earth System Sciences, Brussels, Belgium

[3]Laboratoire des Sciences de l'Environnement Marin (LEMAR), Université de Brest, CNRS, IRD, UMR 6539, IUEM; Technopôle Brest Iroise, Place Nicolas Copernic, F-29280 Plouzané, France

[4]INSU-CNRS, UMR8187 LOG, Laboratoire d'Océanologie et de Géosciences, Université du Littoral Côte d'Opale, ULCO, 32 avenue Foch, 62930 Wimereux, France

[5]Earth Sciences Department, Royal Museum for Central Africa, Leuvensesteenweg 13, Tervuren, B 3080, Belgium

[6]Sorbonne Universités (UPMC, Univ Paris 06)-CNRS-IRD-MNHN, LOCEAN Laboratory, 4 place Jussieu, F-75005 Paris, France

Corresponding author: stephanie.jacquet@mio.osupytheas.fr

Abstract

We report on the zonal variability of mesopelagic particulate organic carbon remineralization and deep carbon transfer potential during the Kerguelen Ocean and Plateau compared Study 2 expedition (KEOPS 2; Oct.-Nov. 2011) in an area of the Polar Front supporting recurrent massive blooms from natural Fe fertilization. Mesopelagic carbon remineralization (MR) was assessed using the excess, non-lithogenic particulate barium (Ba_{xs}) inventories in mesopelagic waters and compared with bacterial production (BP), surface primary production (PP) and export production (EP). Results for this early season study are compared with results obtained during a previous study (2005; KEOPS 1) for the same area at a later stage of the phytoplankton bloom. Our results reveal the patchiness of the season advancement and of the establishment of remineralization processes between plateau (A3) and Polar Front sites during KEOPS 2. For the Kerguelen plateau (A3 site) we observe a similar functioning of the mesopelagic ecosystem during both seasons (spring and summer), with low and rather stable remineralization fluxes in the mesopelagic column (150-400 m). The shallow water column (~500m), the lateral advection, the zooplankton grazing pressure and the pulsed nature of the POC transfer at A3 seem to drive the extend of MR processes on the plateau. For deeper stations (>2000 m) located on the margin, inside a Polar Front meander, as well as in the vicinity of the Polar Front, east of Kerguelen, remineralization in the upper 400 m in general represents a larger part of surface carbon export, but when considering the upper 800 m, in some cases, the entire flux of exported carbon is remineralized. In the Polar Front meander, where successive stations form a time series, two successive events of particle transfer were evidenced by remineralization rates: a first mesopelagic and deep transfer from a past bloom before the cruise, and a second transfer expanding at mesopelagic layers during the cruise. Regarding the deep carbon transfer efficiency, it appeared that above the plateau (A3 site) the mesopelagic remineralization was not a major barrier to the transfer of organic matter to the sea-floor (close to 500 m). There the efficiency of carbon transfer to the bottom waters (>400 m) as assessed by PP, EP and MR fluxes comparisons reached up to 87% of the carbon exported from the upper 150 m. In contrast, at the deeper locations mesopelagic remineralization clearly limited the transfer of carbon to depths >400 m. For sites at the margin of the plateau (station E-4W) and the Polar front (station F-L), mesopelagic remineralization even exceeded upper 150 m export, resulting in a null transfer efficiency to depths >800 m. In the Polar Front meander (time series), the capacity of the meander to transfer carbon to depth >800 m was highly variable (0 to 73 %). The highest carbon transfer efficiencies in the meander are furthermore coupled to intense and complete deep (>800 m) remineralization, resulting again in a close to zero deep (>2000 m) carbon sequestration efficiency there.

Key Words: particulate barium, mesopelagic carbon remineralization, carbon transfer efficiency, Southern Ocean

1. INTRODUCTION

While numerous artificial (Boyd et al., 2000, 2004; Gervais et al., 2002; Buesseler et al., 2004, 2005; de Baar et al., 2005; Hoffmann et al., 2006; Boyd et al., 2012; Smetacek et al., 2012) and natural (Blain et al., 2007; Pollard et al., 2009; Zhou et al., 2010, 2013) ocean iron-fertilization experiments in the Southern Ocean demonstrated the role of iron in enhancing the phytoplankton biomass and production in high-nutrient low-chlorophyll (HNLC) regions, determining to what extent fertilization could modify the transfer of particulate organic carbon (POC) to the deep ocean is far from being comprehensively achieved (Lampitt et al., 2008; Morris and Charette, 2013; Le Moigne et al., 2014; Robinson et al., 2014). This is partly due to the short term over which the observations were made, precluding extrapolation to longer time scales. Moreover, when assessing whether Fe-supply could induce vertical POC transfer, the magnitude of the export from surface is not the only important parameter to take into account. Indeed, POC fate in the mesopelagic zone (defined as 100-1000 m depth layer) is often largely overlooked although these depth layers are responsible for the remineralization of most of the POC exported from the surface layer (Martin et al., 1987; Longhurst, 1990; Lampitt and Antia, 1997; François et al., 2002; Buesseler et al., 2007b; Buesseler and Boyd, 2009). Only few studies considered mesopelagic carbon (C) remineralization rates (Buesseler et al., 2007a; Jacquet et al., 2008a, 2008b, 2011a, 2011b; Salter et al., 2007) to estimate the response of deep POC export to fertilization. Assessing mesopelagic C remineralization is pivotal to evaluate remineralization length scale as well as the time scale of the C storage in the deep ocean. Indeed the typical depth of the main thermocline, 1000 m (IPCC, WG1, 2007, chp5) is often referred to as the horizon clearly removed from the surface ocean and atmosphere (Passow and Carlson, 2012). Overall, assessing mesopelagic C remineralization will allow to better quantify the ocean's biological carbon pump and its efficiency in the global C cycle which bears large uncertainty and is currently under debate (e.g. from 5 Gt/yr in Henson et al., 2011 to 21 Gt C/yr in Laws et al., 2000 and 13 Gt/yr in IPPC WG1 report (ch. 6, 2013).

The present work aims at understanding the impact of a natural iron-induced bloom on the mesopelagic POC remineralization and zonal variability in the Kerguelen area (Southern Ocean). Here, C remineralization was assessed from particulate biogenic Ba (hereafter called excess-Ba or Ba_{xs}; mainly forms as barite $BaSO_4$ crystals) contents in the mesopelagic water column. The link between barite and C remineralization resides in the fact that this mineral precipitates inside oversaturated micro-environments (biogenic aggregates) during the process of prokaryotic degradation of sinking POC (Dehairs et al., 1980, 1992, 1997, 2008; Stroobants et al., 1991, Cardinal et al., 2001, 2005; Jacquet et al., 2007, 2008b, 2011a; Planchon et al., 2013; Sternberg et al. 2007, 2008a, 2008b). Once the aggregates have been remineralized, barites are released and spread over the mesopelagic layer. Overall, earlier work highlights the fact that suspended barite in mesopelagic waters builds up over the growing season and reflects past remineralization activity integrated over several days to weeks (Dehairs et al., 1997; Cardinal et al., 2005; Jacquet et al., 2007, 2008b). An algorithm relating mesopelagic Ba_{xs} contents to oxygen consumption (Shopova et al., 1995; Dehairs et al., 1997) allowed remineralization of POC fluxes to be estimated for the mesopelagic layer. Combined with surface C production and export estimates, mesopelagic Ba_{xs} also informs on the efficiency of the system toward deep carbon transfer. From earlier studies, the efficiency of C transfer through the mesopelagic layer was reported to increase under artificially induced (EIFEX; Strass et al., 2005; Smetacek et al., 2012) and natural (KEOPS; Blain et al., 2007) Fe-replete conditions (Jacquet et al., 2008a, 2008b; Savoye et al., 2008) compared to Fe-limited, non-bloom, HNLC reference stations in the Southern Ocean. In contrast, C transfer efficiency through the mesopelagic layer was reported smaller in natural Fe-replete locations during the SAZ-Sense cruise off Tasmania (Jacquet et al., 2011a, 2011b). Differences in plankton community structure and composition (e.g. diatoms vs. flagellates, type of diatoms) were pointed at, as possible causes of such discrepancies in C transfer efficiency through the mesopelagic layer (Jacquet et al., 2008a, 2011a, 2011b). Also, differences in integration time scales for the processes that control the carbon fluxes in artificially vs. naturally Fe fertilized systems, may yield an incomplete picture of the C transfer potential and lead to misleading conclusions.

Here, we examine changes in mesopelagic POC remineralization during the early spring (Oct. –Nov. 2011) KEOPS 2 expedition to the naturally iron fertilized area eastward of Kerguelen Islands. The hydrographic structure of the Kerguelen area generates contrasted environments that are differently impacted by iron availability and mesoscale activity. The specific objectives of the present work are to assess the zonal variability of mesopelagic C remineralization and deep C transfer potential, and to identify possible causes inducing this variability. As the same area was visited earlier in 2005 during summer at a late stage of the bloom (KEOPS 1; Jan.-Feb., 2005), this condition offers a unique opportunity to estimate the main carbon fluxes over most of the growth season. Mesopelagic C remineralization estimates are compared to particle and biological parameters as reported in other papers included in this issue (Cavagna et al., 2014; Christaki et al., 2014; Dehairs et al., 2014; Lasbleiz et al., 2014; Laurenceau-Cornec et al., 2014; Planchon et al., 2014; Van der Merve et al., 2015) and in Blain et al., (2007); Christaki et al. (2008); Jacquet et al., (2008a); Park et al., (2008); Savoye et al., (2008).

2. EXPERIMENT AND METHODS

2.1. Study area

The KEOPS 2 (Kerguelen Ocean and Plateau compared Study) cruise was conducted in austral spring at the onset of the bloom from 10 October to 20 November aboard the R/V *Marion Dufresne* (TAAF/IPEV). The KEOPS 2 expedition studied the Kerguelen Plateau area (Indian sector of the Southern Ocean) which is characterized by the passage of the Polar Front (PF), as illustrated in Fig.1a. The Kerguelen Plateau is surrounded by the Antarctic Circumpolar Current (ACC) whose main branch circulates to the north of the plateau (Park et al., 2008). A second branch of the ACC circulates to the south of Kerguelen Islands to further join a branch of the Fawn Trough Current (FTC). The FTC has a main northeast direction, but a minor branch splits away northwestward to join the eastern side of the Kerguelen plateau (Park et al., 2008; Fig1.a). These particular hydrographic features generate a mosaic of recurrent massive bloom patterns in the northeastern part of the Plateau and the possible sources and mechanisms for fertilization were investigated during ANTARES 3 (1995; Blain et al., 2001) and KEOPS 1 cruise, later referred to as KEOPS 1 (Jan.-Feb. 2005, late summer conditions; Blain et al., 2007, 2008). During KEOPS 2 the evolution of Chl-a data based on multi-satellite imagery of the study area revealed the presence of different Chl-a rich plumes (D'ovidio et al., 2014) (Fig.1a; e.g. Chl-a map from 11/11/2011). Stations were sampled in distinct zones covering these different bloom patterns (Fig.1a) (corresponding stations are reported in Fig1.b): (a) on the shallow plateau (station A3; see 1 in Fig.1a). Note that station A3 coincides with a site studied during the KEOPS 1 cruise, and that it was sampled twice over a 27-day period; (b) in a meander formed by a quasi-permanent retroflection of the Polar Front (PF) and topographically-steered by the eastern escarpment (Gallieni Spur) of the Kerguelen Plateau (mainly stations E, sampled as a quasi-lagrangian temporal series) (see 2 in Fig.1a); (c) along a North-South Transect (referred to as TNS stations; see 3, grey line in Fig.1a) and a West-East Transect (referred to as TEW stations; see 4, grey line in Fig.1a), both crossing the PF; and (d) in the Polar Front Zone (PFZ) in the vicinity (east) of the PF (station F-L; see 5 in Fig.1a). Furthermore we also sampled a reference HNLC/non bloom/non Fe-fertilized station southwest of the Plateau (station R-2; see 6 in Fig.1a). Station locations are given in Table 1.

Detailed descriptions of the complex physical structure of the area, circulation, water masses and fronts are given in Park et al. (2014). Briefly, the main hydrodynamic features observed during the cruise are the following (see θ–S diagram, Fig.2a): (1) North of the PF, stations in the PFZ (TNS-1, TEW-8 and F-L) present Antarctic Surface Waters (AASW; θ≃ 4°C and density <27); θ–S characteristics between 150 to 400 m at station F-L (and to a lesser extent at station TNS-1) reveal the presence of interleaving with waters from northern (subantarctic) origin, centered between the 27.2 and 27.5 density curves, where Antarctic Intermediate Waters (AAIW) are usually found. This contrasts with the situation at station TEW-8, where there is no evidence of interleaving; (2) stations south of the PF exhibit subsurface temperature minima characteristic of Winter Waters (WW); below the WW three water masses can be identified, namely: the Upper (temperature maximum) and Lower (salinity maximum) Circumpolar Deep Water (UCDW and LCDW), and the Antarctic Bottom Water (AABW). Theses water masses are present roughly in the following depth intervals: 700 m<UCDW< 1500 m; 1500 m <LCDW<2500 m; AABW>2500 m.

Based on the θ–S characteristics (Fig.2a, -2b) and surface phytoplankton biomasses we can schematically group the stations as follows. The R-2 HNLC reference station (white dot in Fig.1b) is characterized by a very low biomass (with low iron contents; Quéroué et al., 2014). Stations TEW-3 and TNS-8 (black dots) are characterized by a low to moderate biomass and Fe contents. Stations A3 and E-4W (red dots; south of the PF) as well as stations TNS-1, F-L and TEW-8 (blue dots; north of the PF) are characterized by high biomass and iron contents. Stations in the core of the PF meander (green dots; stations TNS-6, E-1, E-2, E-3, E-4E and E-5 considered as a temporal series) are characterized by moderate biomass and iron contents.

2.2. Sampling and analyses

22 CTD casts (surface to 500-2000 m) were sampled for particulate barium (Table 1) using a CTD-rosette equipped with 22 12L Niskin bottles. Deep particulate Ba profiles (>1000 m) were not systematically obtained from the same CTD cast, but from successive casts sampled closeby in time and space and having similar θ-S data profiles. In the following, we use both the station and CTD numbers to refer to stations.

4 to 7 L of seawater were filtered onto 47 mm polycarbonate membranes (0.4 µm porosity) under slight overpressure supplied by filtered air (0.4 µm). The filters were rinsed with Milli-Q grade water (<5 mL) to remove sea salt, dried (50°C) and stored in Petri dishes for later analysis. In the home-based laboratory we performed a total digestion of samples using a tri-acid (0.5 mL HF/1.5 mL HCl/1 mL HNO_3; all Suprapur grade) mixture in closed telfon beakers overnight at 90°C in a clean pressurized room. After evaporation close to dryness samples were re-dissolved into around 13 mL of HNO_3 2%. The solutions were analysed for Ba and other major and minor elements by ICP-QMS (inductively coupled plasma-quadrupole mass spectrometry; X Series 2 ThermoFisher) equipped with a collision cell technology (CCT). To correct instrumental drift and matrix effects, internal standards and matrix-matched calibrations were used. We analysed several certified reference materials which consisted of dilute acid-digested rocks (BHVO-1, JB-3 and JGb-1), natural riverine water (SLRS-5) and multi-element artificial solutions for these external calibrations. Based on analyses of these external standards, accuracy and reproducibility are better than ± 5%. For

more details on sample processing and analysis we refer to Cardinal et al. (2001). Among all elements analysed, particular interest went to Ba and Al. The presence of sea-salt was checked by analysing Na and the sea-salt particulate Ba contribution was found negligible. Average detection limits equal 0.6 nM for Al and 3 pM for Ba. Detection limits were calculated as three times the standard deviation on the blank measured on board and then normalized to an average dilution factor of 385, i.e., particles from around 5 L of Milli-Q water, dissolved in a final volume of 13 mL as for the samples. Biogenic barium (hereafter called excess-Ba or Ba_{xs}) was calculated as the difference between total particulate Ba and lithogenic Ba using Al as the lithogenic reference element (Dymond et al., 1992; Taylor and McLennan, 1985). At most sites and depths the biogenic Ba_{xs} represented >95% of total particulate Ba. Lithogenic Ba reached up to 20% of total particulate Ba at some depths in the upper 80-100 m, mainly at station R-2 and stations north of the Polar Front (i.e., TEW-8, F-L and TNS-1). The standard uncertainty (Ellison et al., 2000) on Ba_{xs} data ranges between 5 and 5.5%. Ba_{xs} and Al data are reported in Appendix A.

2.3. O_2 consumption and POC remineralization

The rate of oxygen consumption and particulate organic carbon remineralization rate in the mesopelagic layer (later referred to as MR) can be estimated using an algorithm relating mesopelagic Ba_{xs} contents and oxygen consumption based on earlier observations in the Southern Ocean (Shopova et al., 1995; Dehairs et al., 1997; 2008). The detailed calculations are described in Jacquet et al. (2008a, 2011a). Briefly, we use the following equations:

$$J_{O_2} = (Ba_{xs} - Ba_{residual})/17450 \qquad \text{(Eq.1)}$$

$$C_{respired} = Z \times J_{O_2} \times RR \qquad \text{(Eq.2)}$$

where J_{O2} is the O_2 consumption (µmol l^{-1} d^{-1}) and $C_{respired}$ is the Mineralization Rate of organic carbon (in mmol C m^{-2} d^{-1}; MR); Ba_{xs} is the depth-weighted average Ba_{xs} value (DWAv), i.e. the Ba_{xs} inventory divided by the depth layer considered Z, $Ba_{residual}$ is the residual Ba_{xs} signal (or Ba_{xs} background) at zero oxygen consumption and RR is the Redfield C/O_2 molar ratio (127/175; Broecker et al., 1985). DWAv Ba_{xs} values were calculated both for the 150 to 400 m (Plateau and deep stations) and the 150 to 800 m layers (deep stations only) (see details further below). The residual Ba_{xs} is considered as 'preformed' Ba_{xs}, left-over after partial dissolution and sedimentation of Ba_{xs} produced during a previous phytoplankton growth event. In $BaSO_4$ saturated waters, such as the ones filling the whole ACC water column (Monnin et al. 1999), this background Ba_{xs} value was considered to reach 180 to 200 pM which is rather characteristic for the deep ocean (>1000m) (see Dehairs et al., 1997; Jacquet et al., 2008a, 2011). In the present study we used a Ba_{xs} background of 180 pM.

We take the opportunity here to also compare O_2 consumption rates for the KEOPS 1 expedition (D. Lefèvre, unpublished data) with KEOPS 1 Ba_{xs} data published earlier (Jacquet et al., 2008a). No such O_2 consumption data are available for KEOPS 2. During KEOPS 1, dark community respiration (DCR) was estimated from changes in the dissolved oxygen concentration over 72 hours incubations. Discrete samples were collected at three depths in the mesopelagic zone from Niskin bottles into 125 cm^3 borosilicate glass bottles according to the WOCE procedure, and oxygen concentration was determined by Winkler titrations using a photometric endpoint detector (Williams and Jenkinson, 1982). By integrating DCR data in the water column we estimated the rate of oxygen consumption (later referred to as JO_2-W). We compared JO_2-W obtained from incubated oxygen samples with the rate of oxygen consumption based on KEOPS 1 mesopelagic Ba_{xs} contents (Eq.1; later referred to as JO_2-Ba). Dissolved oxygen was measured three times at station A3 (same location as during KEOPS2) over a 19-day period (A3 CTD #32, #74 and #119). Dissolved oxygen was also measured at station C11 located off-shelf in less productive HNLC waters (51.65°S, 78.00°E; not shown in Fig.1) and was sampled two times over a 10-day period (C11 CTD#42 and #83). Fig.3 compares JO_2-W and JO_2-Ba for repeat stations A3 (#32, 74 and 119) and C11 (#42 and 83) (integration between 150-300 m). JO_2-W range from 0.082 to 0.208 mmol m^{-2} d^{-1} at station A3 and from 0.292 to 0.528 mmol m^{-2} d^{-1} at station C11. Although JO_2-Ba rates (from 0.846 to 1.555 mmol m^{-2} d^{-1}) are slightly higher than JO_2-W, JO_2 rates are of the same order of magnitude and present a same trend. We observe a significant positive correlation between both JO_2 rates (R^2=0.90; p<0.01) with a slope of 0.64. The difference in oxygen consumption rates could be explained by the integration time of both methods (few hours for the incubations vs. few days to weeks for Ba_{xs}) and by the fact that KEOPS 1 occurred at the decline of the bloom (late summer; low organic substrates), which would explain the lower JO_2 rates as estimated by the incubation method.

Overall, these results highlight the need for further constraining spatial and temporal variability of deep ocean oxygen utilisation via a combination of direct rate measurements and the Ba_{xs} proxy. In the present work O_2 consumption and POC remineralisation was assessed from Ba_{xs} inventories and Eqs.1 and 2. C remineralization rates are given in Table 1. Relative standard uncertainties (Ellison et al., 2000) on C remineralization ranged between 4 and 20%.

3. RESULTS

3.1. Particulate biogenic Ba_{xs} profiles

Ba_{xs} profiles in the upper 800 m are reported in Fig.4. The complete whole water column data set is given in Appendix A. From previous studies we know that Ba_{xs} in surface waters is distributed over different, mainly non-barite biogenic phases (see Stroobants et al., 1991, Jacquet et al., 2007, Cardinal et al., 2005, Sternberg et al., 2005). As such, these do not reflect POC remineralization processes, in contrast to mesopelagic waters where Ba_{xs} is mainly composed of barite (Dehairs et al., 1980) formed during prokaryotic degradation of sinking POC (Martin et al., 1987; Sarmiento et al., 1993; Buesseler et al., 2007b). For KEOPS 2 we observe that Ba_{xs} concentrations generally increase below 150 m (i.e., they increase above the background level set at 180 pM), but some sites have ocean surface Ba_{xs} contents significantly larger than background (E-1,896 pM at 21 m; E4-E, 563 pM at 93 m). Such values are not unusual, and very high surface values have been observed occasionally in earlier Southern Ocean studies. During KEOPS 1, surface Ba_{xs} maxima at the three A3 repeats stations ranged from 1354 to 5930 pM at 50 m, likely associated with phytoplankton derived particles (Jacquet et al., 2008a).

The following part focuses on the mesopelagic zone where most of the remineralization of exported organic matter takes place. The Ba_{xs} profile for station R-2 (CTD #17) displayed a characteristic mesopelagic Ba_{xs} maximum reaching up to 834 pM at 304 m which is actually one of the highest values observed for the whole study (Fig.4a). Ba_{xs} profiles for stations A3 above the Kerguelen plateau (A3-1 CTD #4 and A3-2 CTD #107; Fig.4b) had lower mesopelagic Ba_{xs} contents, with values ranging from about 80 to 350 pM. For both A3 visits, Ba_{xs} values increased close to the seafloor reaching up to 1108 pM (A3-1, 474 m) and 1842 pM (A3-2, 513 m). In contrast, station E-4W (located further north along the margin in deeper waters, but with similar θ–S and Chl-a characteristics as station A3) displayed a large mesopelagic Ba_{xs} maximum reaching up to 627 pM at 252 m (Fig.4c). Station TEW-3 (located on the Kerguelen plateau, in waters with similar θ–S and Chl-a characteristics as station TNS-8) had a profile similar to the one observed at station A3-2, but compared to plateau sites A3-1 and A3-2 no increased Ba_{xs} contents were observed in bottom water (Fig.4d). The other stations of the study area (Fig.4d-g) have Ba_{xs} profiles similar to the one at station E-4W, showing the characteristic Ba_{xs} maximum between 200 and 500 m. Note that for most of the stations, Ba_{xs} concentrations in waters below the mesopelagic maximum did not systematically decreased to reach the Ba_{xs} background level (180 pM; see above). In some cases Ba_{xs} contents significantly higher than residual Ba_{xs} were observed until below 1000 m (see Appendix A). This is particularly salient at stations TNS-6, E-1, E-2 and F-L where Ba_{xs} values below 1000 m reach 410 pM at 1886 m (TNS-6) and 436 pM at 1498 m (E-1). These cases of high deep Ba_{xs} contents clearly contrasted with the values observed at station E4-E (Fig.4h).

3.2. Depth-weighted average Ba_{xs} content of mesopelagic waters

Since the base of the mixed layer was generally shallower than ≤150 m, this depth is taken as the upper boundary of the mesopelagic domain. The depth-weighted average (DWAV) Ba_{xs} contents, calculated for the 150-400 m and 150-800 m depth intervals, are given in Table 1. For the profiles on the plateau (500 m water column) bottom waters with evidence of sediment resuspension were not taken into account when calculating DWAv Ba_{xs} values (≥ 400 m). Particle size spectra indicated that sediment resuspension occurred especially at stations A3 and TEW-3 (Jouandet et al., 2014; Lasbleiz et al., 2014; Van der Merve et al., 2015;). Thus, at site A3 (Fig.4b) DWAV Ba_{xs} was calculated for the layer between 150 and 354 m for A3-1 (CTD #4) and between 150 and 405 m for A3-2 (CTD#107). For station TEW-3 (CTD #38) DWAV Ba_{xs} was calculated for the water layer between 150 and 400 m (Fig.4d). For the deep sites, we considered both, the 150-400 m and the 150-800 m depth intervals, when calculating the DWAV Ba_{xs} contents. Depth weighted average Ba_{xs} values were translated into carbon remineralization rates using equation (1) and (2) given above. These rates ranged from 2 to 91 mgC m^{-2} d^{-1} (Table 1).

DWAV Ba_{xs} values range from 199 to 572 pM (Table 1) and fit within the range reported for Polar Front areas during previous studies (Cardinal et al., 2001, 2005; Jacquet et al., 2005, 2008a, 2008b, 2011; Planchon et al., 2013). For the KEOPS 2 cruise the main observed features are:

(a) Unexpectedly, the highest DWAV Ba_{xs} value of the whole study area (572 pM; 150-400 m) was observed at the reference R-2 site. Bowie et al. (2014), Quéroué et al. (2014) and van der Merve et al. (2015) reported for R-2 local maxima in particulate and dissolved trace metals at 500 m and deeper, reflecting lateral transport of lithogenic matter possibly originating from the Leclaire Rise (a large seamount located west of R-2). Similarly, Lasbleiz et al. (2014) observed a maximum of lithogenic silica (LSi) at 500 m, confirming lithogenic inputs there. However, we note that the mesopelagic Ba_{xs} maximum at R-2 occurs at shallower depths, around 300 m, and that there is no evidence for elevated values at 500 m where the previous authors reported higher trace element and silica concentrations. Also, as reported above (see section 2.2 and Appendix A), the higher lithogenic Ba fractions at R-2 (up to 20% of the total Ba) occur only in the upper 80 m. Moreover, we do note that surface waters at R-2 experienced already some nitrate consumption as compared to subsurface Winter Waters (Tmin waters). Indeed, surface waters had 10% less nitrate than Winter Water (26 µM at 5 m vs. 29 µM at 200 m) and the isotopic enrichment of this surface nitrate confirmed an imprint of uptake (see Dehairs et al., 2014). Also, Lasbleiz et al. (2014) report relatively low Si:C and Si:N ratios for surface ocean suspended matter) pointing to the development of a diatom assemblage just prior the sampling, consistent with the high dissolution rates of biogenic silica (BSi) Closset et al. (2014) report for R-2 surface waters. It is therefore likely that the mesopelagic Ba_{xs} content at R-2 indeed reflects remineralization of organic material that was fuelled by an important past early spring production and export event. Similarly, F. Dehairs (unpublished results) observed the presence of significant numbers of barite microcrystals in mesopelagic waters at the KERFIX time series station (50°40'S, 68°25'E) located east of R-2 during late winter (Nov. 1993). Results would thus suggest the occurrence in this HNLC area of recurrent brief early spring diatom productive period pulses and subsequent export and remineralization activity in the underling layers. Chla satellite images (Giovani online Visualization and Analysis system, NASA GES DISC) corroborate that the R-2 and KERFIX area is occasionally subject to enhanced biomass during early spring;

(b) The two successive visits (27-day interval) at site A3 yielded relatively low DWAV Ba_{xs} values of 267 and 316 pM, and a quite similar value was observed for the shallow station TEW-3 (324 pM), located further north on the plateau, but north of the PF. Note that for comparison purposes, we recalculated the DWAV Ba_{xs} and MR values of KEOPS 1 by considering upper and lower mesopelagic layer boundaries of 150 and 400 m rather than 125 and 450 m, as in Jacquet et al. (2008a). Also, in the latter study the high Ba_{xs} contents observed near the seafloor were not excluded from the calculations, while they are here. These increased benthic boundary layer Ba_{xs} contents (observed also during KEOPS 2) are due to sediment resuspension which extended up to 70 m above the seafloor during KEOPS 1 (Blain et al., 2008; Venchiarutti et al., 2008; Armand et al., 2008). Because of these slightly different depth intervals over which Ba_{xs} values were integrated, the KEOPS 1 values discussed here will be slightly different from those reported in Jacquet et al. (2008a). At the other depths the lithogenic Ba contribution at A3 (KEOPS 2) was only minor;

(c) The time series stations in the Polar Front meander had DWAV Ba_{xs} contents ranging from 258 to 427 pM (150-400 m), so reaching values exceeding those on the plateau. For these time series stations values decreased between day 0 (TNS-6) and 12 (E-3), and then increased again at days 22 (E-4E) and 27 (E-5). Stations E-4W and TNS-8 above the plateau but in deeper waters close to the Kerguelen margin, at the edge the high biomass plume (Figure 1) had the highest DWAV Ba_{xs} values (468 and 473 pM, respectively; 150-400 m), not considering the R-2 reference station. The Polar Front F-L site, although located within the eastern part of the high biomass plume had a smaller DWAV Ba_{xs} value of 345 pM (150-400 m) and the close by station TEW-8 had the lowest DWAV Ba_{xs} value of the whole study area (199 pM; 150-400 m).

4. DISCUSSION

4.1. Mesopelagic Ba_{xs} and bacterial production

Previous studies revealed that the shape of the column-integrated bacterial production (BP) profile (i.e. the attenuation length scale) was important in setting the Ba_{xs} signal in the mesopelagic zone (Dehairs et al., 2008; Jacquet et al., 2008a, 2011a). Mesopelagic Ba_{xs} content is smaller when most of the column integrated BP is restricted to the upper mixed layer (indicating an efficient, close to complete remineralization within the surface), compared to situations where a significant part of integrated BP was located deeper in the water column (reflecting significant deep bacterial activity and POC export). During KEOPS 2 the incorporation of ^{3}H-leucine was used to estimate bacterial production. BP data are described in Christaki et al. (2014). In Fig.5 we compare column-integrated BP at 150 m over 400 m (BP150/400) and DWAV Ba_{xs} for the 150-400 m depth interval, next to the relation obtained during KEOPS 1 (BP200/125 and 150-450 m DWAV Ba_{xs}; Jacquet et al., 2008a; Christaki et al., 2008). Excluding stations A3, E-1, E-2 and E-3, KEOPS 2 data presented a significant correlation (R^2=0.88; p<0.01) and a similar trend to the one reported for KEOPS 1. A similar picture was obtained when integrating DWAV Ba_{xs} and BP up to 800 m (not shown). The time series

"E" stations in the meander revealed a shift from stations E-1, E-2 and E-3 to stations E-4E and E-5, i.e. towards the trend reported above. A shift was also apparent at station A3 from KEOPS 2 (early spring) to KEOPS 1 (late summer). It is thus possible that results reflect the occurrence of different stage of bloom advancement. The large variability of Ba_{xs} and BP relationship during KEOPS 2, especially at A3 site and in the meander, could reflect the temporal evolution and patchiness of the establishment of mesopelagic remineralization processes in this Polar Front area.

4.2. Fate of exported organic C in the mesopelagic zone and deep water column

An important question relates to the fate of the exported POC: how much of this POC is respired in the mesopelagic waters and how much escapes remineralization and is exported to deeper layers where longer term sequestration is likely (see e.g. Passow and Carlson, 2012; Robinson et al., 2014; Schneider et al., 2008). To address these questions, we defined two ratios: (1) the mesopelagic C remineralization efficiency (r-ratio in Table 2) which is the ratio of mesopelagic C remineralization (MR, based on the DWAV Ba_{xs} concentrations) over C export (EP) from the 150 m horizon (based on ^{234}Th, see Planchon et al., this issue), and (2) the C transfer efficiency at 400 and 800 m (i.e., T400, T800 in Table 2) which is the fraction of C export (EP) at 150 m passing through the 400 m (T400) or the 800 m (T800) horizons (e.g., T400= EP400/EP150 = 1–(MR/EP150), with MR/EP150 = r-ratio; see above). This approach is similar to the one developed by Buesseler and Boyd (2009) stating that a conventional curve-fitting of particle flux data (i.e., power law or exponential) skews our interpretation of the mesopelagic processes. They recommended the use of combined metrics to capture and compare differences in flux attenuation. In the following, we compare MR fluxes for the different KEOPS 2 areas (Reference site; Plateau sites; Polar

Front and Polar Front Meander) and discuss remineralization and transfer efficiencies for those sites for which MR, primary production (PP) and/or EP data (Table 2) were available. PP data were estimated from uptake experiments including 24-hour incubations at different PAR levels over the euphotic layer i.e., up to the 0,01% PAR level (Cavagna et al., 2014). EP data were estimated from ^{234}Th activities and ^{234}Th /POC ratios and are discussed in Planchon et al. (2014). The thorium method integrates POC export over a 1 month period (^{234}Th half live equals 24.1 days). We remind here that MR fluxes as based on mesopelagic Ba_{xs} reflect past remineralization activity integrated over several days to a few weeks (Dehairs et al., 1997; Cardinal et al., 2005; Jacquet et al., 2007, 2008b). In order to compare EP with MR (r-ratio and transfer efficiency) we consider EP fluxes from 150 m. Results are compared with late summer KEOPS 1 results. For KEOPS 1, PP data are detailed in Lefèvre et al. (2008) and Mosseri et al. (2008), EP data are detailed in Savoye et al. (2008) and Ba_{xs} data are described in Jacquet et al. (2008a).

4.2.1. Reference station R-2

Since station R-2 had the highest DWAV Ba_{xs} content it yielded the highest MR flux of the whole study area (91 mgC m^{-2} d^{-1}; 150-800 m; Table 2). In contrast, both PP and EP fluxes at R-2 were very low (132 and 10 mgC m^{-2} d^{-1}, respectively) and the calculated MR flux exceeded EP (Table 2). The resulting export efficiency (EP/PP) was high, and T400 and T800 value (the fraction of EP exported deeper than 400 m and 800 m, as defined above) equal 0 (i.e., no export of POC beyond 400 and 800 m; note that >100% values, i.e., MR>EP, were set to zero in Fig.7a and Table 2). The fact that MR exceeds EP therefore implies a non-steady state condition at the R-2 site. As reported above, R-2 probably experienced a brief early spring diatom production pulse days to a few weeks before the start of the KEOPS 2 cruise, followed by subsequent export and quite important remineralization activity in the underling layers as depicted by MR data.

4.2.2. Station A3 on the Plateau

The MR fluxes on the plateau varied little between the two visits 27 days apart (Table 1) and as discussed below they were moreover similar to summer values obtained during KEOPS 1 (see Jacquet et al., 2008a) when the same A3 site was sampled 3 times over a 19-day period. While during KEOPS 2 (spring) MR fluxes at A3 ranged from 11 to 14 mgC m^{-2} d^{-1} (with a standard uncertainty around 5%) they were slightly larger during KEOPS 1 (summer; 17 to 23 mgC m^{-2} d^{-1}) (Fig.5). We observed differences in the mesopelagic POC remineralization efficiency between the two seasons (r-ratio, blue values in Fig.6, Table 2). During KEOPS 1 r-ratios (MR/EP) remained low, ranging from 7 to 9% of EP at A3, while during KEOPS 2 r-ratios were slightly higher but decreased from 29% (A3-1; first visit) to 13%, 27 days later (A3-2; second visit). This variation in r-ratio during KEOPS 2 is mostly due to an increase of EP (from 47 to 85 mgC m^{-2} d^{-1}; Planchon et al., 2014) over the same period while MR showed little change. Although at this early stage of the season (spring) PP at A3-2 had already reached 2172 mgC m^{-2} d^{-1} (Cavagna et al., 2014), EP remained relatively low (85 mgC m^{-2} d^{-1}). Here EP accounted for only about 4% of PP (low export efficiency; see green data points in Fig.5). This condition suggested that phytoplankton biomass was accumulating in the surface waters without significant export yet, or that C was channeled to higher trophic levels as suggested by Christaki et al. (2014). Note that a negative relationship between primary productivity and surface carbon export efficiency has already been reported from previous studies in the Southern Ocean (Savoye et al., 2008; Morris et al., 2007; Jacquet et al., 2011a; 2011b; Lam et al., 2007). Among possible explanations for the occurrence of high productivity-low export efficiency regimes in high latitude systems Maiti et al. (2013) mentioned differences in trophic structure, grazing intensity, recycling efficiency, high bacterial activity, or increase in DOC export, but the exact reason remain unclear. In contrast, during KEOPS 1 (summer), EP fluxes reached 250 mgC m^{-2} d^{-1} at 125 m (14-31% of PP) while PP ranged from 865 to 1872 mgC m^{-2} d^{-1}, reflecting enhanced export efficiency (Jacquet et al., 2008a; Savoye et al., 2008).

It is important to underline the fact that MR at station A3 was only slightly higher in summer than in spring especially considering the large differences in export efficiency between seasons. According to results from sediment traps deployed over one year at the A3 site, Rembauville et al. (this issue-b) reported that 60% of the annual POC export at the base of the mixed layer occurred over a short periods of time representing <4% of the years and was composed by small highly silicified, fast sinking, resting spores of diatoms that bypass grazing pressure. According to these authors, the pulses are linked to nutrient depletion dynamics inducing resting spore formation. During the rest if the year, the flux was composed of small diatoms (empty frustules) and small fecal pellets, with efficient C retention in the surface layer or transfer to trophic levels. If we consider that export conditions during KEOPS 2 are more similar to those prevailing most of the year, it is surprising that during KEOPS 1 (that would reflect an export event toward the end of the growth season) MR is not more important. This would indicate that fast sinking- highly silicified- and pulsed material was directly transferred to the bottom without major remineralization. Note for example that at the complex R-2 reference station, a small export event (Laurenceau-Cornec et al.; this issue) held heavily silicified diatoms (Lasbleiz et al.; 2014), and that the material was efficiently remineralized in the upper mesopelagic layer as witnessed by the high MR values we observe for that station. For the KEOPS 2 A3 site Laurenceau-Cornec et al. (2014) report that the sinking flux collected in the upper layer using gel-filled sediment traps was composed by phytodetrital aggregates that held slightly silicified diatoms (Lasbleiz et al., 2014). Even considering the shift from slightly- to highly-silicified material transfer between spring (KEOPS2) and summer (KEOPS 1), MR only slightly increases between both periods. Also, the mesozooplankton biomass at A3-2 was one of the highest of the KEOPS2 cruise, with a doubling from KEOPS 2 (early spring) to KEOPS 1 (late summer) (Carlotti et al., 2014). It is thus possible that at A3 the export event reported above, combined with a lasting grazing pressure would have induced this rather low and perduring mesopelagic remineralization. We also wonder whether the shallow water column at A3 combined with lateral advection above the plateau would play a role in triggering the mesopelagic POC remineralization activity and in setting its efficiency. For KEOPS 1, Venchiarutti et al. (2008) report that lateral advection over the plateau could significantly impact particle dynamics. During KEOPS 1, station B1 (CTD68) located on the plateau upstream from A3 according to the plateau circulation (Park et al., 2008) exhibited a very similar Ba_{xs} distribution as station A3: low mesopelagic Ba_{xs} and important bottom resuspension (not shown here; see Jacquet et al., 2008a). These strong similarities in Ba_{xs} profiles shape would indicate that next to the pulsed nature of the events, the dynamics on the shallow plateau play an important role in limiting the extend of mesopelagic POC remineralization processes.

In Fig.7a is shown for both KEOPS cruises the ratio of EP over PP (export efficiency) vs. the fraction of EP exported deeper than 400m (i.e. T400; defined above). Note that for station A3-1 (KEOPS 2), there are no PP data. The A3 site shows increasing EP/PP ratios from spring (KEOPS 2) to late summer (KEOPS 1), and so do the T400 values (A3-1: 70%; A3-2: 87%; KEOPS 1 A3 site: 92±1%). Station E-4W located in waters with similar θ-S and Chl-a characteristics as the A3 plateau site but has a deeper water column (1384 m has PP and EP fluxes of the same order of magnitude (Table 2). However, MR values (36 mgC m^{-2} d^{-1}; 150-400 m) are larger at E-4W, resulting in a lower T400 value of around 33%, compared to 87% for A3-2 (Fig.7a). When integrating down to 800 m, T800 at E-4W equals 0 (i.e., no export of POC beyond 800 m; Fig.7a and Table 2). Station F-L (in the vicinity of the PF; 74.7°E) appears to function in a similar way as observed for E-4W (71.4°E). PP at station F-L is relatively high (3380 mgC m^{-2} d^{-1}), while EP is quite low (43 mgC m^{-2} d^{-1}), reflecting the fact that the biomass was not yet exported from the surface waters or was transferred to higher trophic levels. Since MR fluxes are slightly lower (21 mgC m^{-2} d^{-1}; 150-400 m) at F-L than at E-4W, resulting T400 values are higher (52%) there.

Overall, during KEOPS 2 it appears that biomass at stations A3, E-4W and F-L (sites of high productivity) was accumulating in surface waters (e.g. transfer to higher trophic levels) and export did not start yet considering the early stage of the season during KEOPS 2. Our observations allow us to conclude the following:

(1) Both seasons (KEOPS 1 and KEOPS 2) showed a similar functioning of the mesopelagic ecosystem at A3. The rather low and perduring MR fluxes under high production and variable export regimes (high export efficiency during KEOPS 1 and low export efficiency during KEOPS 2) indicated that here mesopelagic remineralization does not represent a major resistance to organic matter transfer to the sea-floor at A3. On average (considering both seasons, but excluding A3-1) the C transfer efficiency into the deep (>400 m) as assessed by PP, EP and MR fluxes comparisons reached 91±3% at A3;

(2) In contrast to A3, E-4W and F-L showed important mesopelagic remineralization rates, reducing the efficiency of C transfer beyond 400 m to 33 and 52%, respectively, and to zero for both stations beyond 800 m. Bottom depth, lateral advection, zooplankton grazing pressure and the pulsed nature of the POC transfer at A3 were the particular conditions that could drive the differences in C transfer efficiency between A3 and E4-W and F-L and limit the extend of MR processes at A3.

4.3. Stations in the meander

Temporal short term changes for the stations TNS-6, E-1, E-2, E-3, E-4E and E-5, located in the Polar front meander, will be discussed in this section. Note that no PP or EP data exist for TNS-6. From Table 2 it appears that PP almost doubled between E-1 and E-5 but this increase was not paralleled by an increase of EP and MR, except for the 30% EP increase from E-1 to E-3. In fact overall EP shows a decreasing trend with time, while MR (150-400 m) stays rather constant, except for the decrease between E-1 and E-3 (Table 2). As reported above such a mismatch may result from differences in time scales characterizing the different processes that were compared. The most likely explanation is that in this early stage of the growth season, phytoplankton biomass was accumulating in the surface layer and export was lagging behind.

The ratio of EP over PP vs. T400 and T800 showed a large variability in transfer efficiency inside the meander (Fig.7b). PP and EP fluxes increased by about 30% from E-1 to E-3, but a concomitant decrease of mesopelagic MR yielded to an enhanced transfer efficiency, from 74 to 92%, through the 400 m boundary and from 52 to 73% through the 800 m boundary. This suggests that significant remineralization should have occured at greater depths (even > 1000 m) and it is also reflected by the presence of Ba_{xs} maxima below 1000 m (see Fig.4h and Appendix A). This was particularly salient when plotting Ba_{xs} contents vs. depths over the 27-day observation period (Fig.8). The high deep water Ba_{xs} values in Figure 8 were not taken into account when integrating TNS-6 and E-1 profiles between 150 and 400 or even 150 and 800 m (Fig. 5e). Considering that the seafloor in the meander area is at about 2000 m depth, it seems unlikely that these high Ba_{xs} contents at depths >1000 m were due to sediment resuspension. Also, particle spectra for these sites do not reveal any bottom resuspension (Jouandet et al., 2014; Lasbleiz et al., 2014; Vandermerve et al., 2015;). Therefore, the high deep (>1000 m) Ba_{xs} contents at TNS-6 and E-1 most likely reflected the fact that here significant remineralization of POC material did occur in the bathypelagic domain and even down to the sea-floor. Note that suspended particles in the depth range containing the deep Ba_{xs} maxima were dominated by the <2 μm size fraction (Zhou et al., pers. comm.). When integrating the Ba_{xs} contents from 150 m to the sea-floor at stations TNS-6 and E-1, MR fluxes increase to 156 and 184 mgC m^{-2} d^{-1} respectively. Such C fluxes were similar to the EP values (maximum value of 130 mgC m^{-2} d^{-1} at E-3) and suggested that the exported POC was entirely remineralized in the water column leaving no C for transfer to the sediments.

Overall, the temporal pattern of mesopelagic remineralization described above reflects two successive events of particle transfer: a first transfer from a previous bloom (occurred before visiting TNS-6 and perduring at E-1) and a second transfer from E-4E to E-5. The first transfer was evident by the downward (up to the bottom) propagation of the mesopelagic Ba_{xs} maximum signal, which mostly weakens at E-2. The second event was reflected by the occurrence again of important mesopelagic Ba_{xs} build-up at E-4E and E-5. Overall, our results indicated the large capacity of the Polar Front Meander to transfer POC material to depth, but in contrast to station A3 on the Plateau, this transfer was coupled to intense and near to complete POC remineralization (as also observed at E-4W and F-L). Between-sites changes in mesopelagic carbon remineralization due to unequal biomass productivity and iron fertilization over the Kerguelen Plateau were thus relatively complex. Furthermore, the situation in the Meander area seems to corroborate results obtained in the iron-replete Subantarctic Zone east of the Tasman Plateau (Australian sector of the Southern Ocean; SAZ-Sense cruise; Jacquet et al., 2011a, 2011b), where the mesopelagic remineralization efficiency was reported relatively high (on average 91%) and the deep (>600 m) carbon transfer weak (<10%). Finally, the important Ba_{xs} contents reported between 1000 and 2000 m during the first stages of the meander time-series strengthen recent results indicating for the Southern Ocean that 1000 m is insufficient as an ocean-wide reference for carbon transfer and sequestration potential (Robinson et al., 2014).

5. Conclusion

Based on spatially and temporally well resolved mesopelagic excess particulate Ba inventories this work estimated mesopelagic POC remineralization above the Kerguelen Plateau and inside a permanent meander of the Polar Front to the east of Plateau, areas. The observed variability of mesopelagic remineralization reflects differences in the fate of the biomass that is exported to the deep ocean, between Plateau and Polar Front. Results also reveal the patchiness of the season advancement and of the establishment of remineralization processes between theses sites. Our results indicate that the reference station R-2 experienced few days to weeks before the start of the cruise an export event that was efficiently remineralized in the upper mesopelagic layer. In terms of deep ocean carbon transfer efficiency, our results highlight that above the plateau (A3 site) mesopelagic remineralization is not a major barrier to organic matter transfer to the sea-floor, with carbon transfer beyond 400 m reaching up to 87% of EP during KEOPS 2, while in the Polar Front Meander remineralization of exported organic carbon in the upper 400 m is more efficient than above the plateau. In the Meander area remineralization may even balance export when including its effect in the deeper waters (till 800 m and even deeper), thus resulting in a close to zero carbon transfer to sediment. A similar condition is also observed for sites at the margin of the plateau (E-4W) and the Polar front (F-L).

Acknowledgements

We thank the officers and crew of R/V *Marion Dufresne* for their assistance during work at sea. We are indebted to chief scientist S. Blain and voyage leader B. Quéguiner for skillful leadership during the cruise and to the CTD team for managing rosette operation and CTD data. This research was supported by the French Agency of National Research grant (project KEOPS 2, #ANR-10-BLAN-0614), the Belgian Science Policy (BELSPO) project 'BIGSOUTH' (SD/CA/05A), Flanders Research Foundation (FWO Project G071512N), the European Union Seventh Framework Programme (Marie Curie CIG 'MuSiCC' under grant agreement n° 294146 to D.C.) and the Strategic Research Programme at Vrije Universiteit Brussel.

Figure captions

Figure 1: (a) Kerguelen Island area in the Southern Ocean with KEOPS 2 sampling zones and MODIS Chlorophyll concentrations (mg m^{-3}) (Chl-a map from 11/11/2011, courtesy F. d'Ovidio) superposed. 1 refers to station A3; 2 to stations E; 3 to the South-North Transect; 4 to the West-East Transect; 5 to station F-L and 6 to reference station R-2; (b) Corresponding stations location. Colors indicate stations with near similar θ–S and Chl-a characteristics.

Figure 2: (a) Potential temperature θ – salinity S plots and isopycnals for KEOPS 2 profiles, (b) Focus on the upper 200 m water column. AASW= Antarctic Surface Waters, AAIW= Antarctic Intermediate Waters, WW= Winter Waters, UCDW and LCDW= Upper and Lower Circumpolar Deep Water, AABW= Antarctic Bottom Water. Graph constructed using Ocean Data View (Schlitzer, 2002; Ocean Data View; http://www.awi-bremerhaven.de/GEO/ODV).

Figure 3: Rates of oxygen consumption (mmol m^{-2} d^{-1}) during KEOPS 1 as directly measured (JO_2-W) and from mesopelagic Ba_{xs} contents (JO_2-Ba). Rates are integrated between 150-300 m.

Figure 4: Particulate biogenic Ba_{xs} profiles (pM) in the upper 800 m (Fig.4a-g) and in the upper 2500 m (Fig.4h). Stations are identified by CTD cast numbers. BKG= Ba_{xs} background (180 pM).

Figure 5: Regression of the ratio of integrated bacterial production (BP) in the upper 150 m over integrated BP in the upper 400 m versus depth weighted average (DWAv) mesopelagic Ba_{xs} (pM; 150-400 m) during KEOPS 2. KEOPS 1 data (dots) are reported for comparison.

Figure 6: Schematic, comparing the fate of POC at station A3 during KEOPS 1 and KEOPS 2 cruises. PP= primary production, EP= export production at 150 m depth and MR= mesopelagic POC remineralization deduced from the Ba_{xs} maxima and integrated between 150-400 m; all fluxes in mgC m^{-2} d^{-1}. EP/PP (green values), MR/PP (red values) and MR/EP (r-ratio, blue values) ratios shown as %.

Figure 7: Y-axis: EP/PP = POC flux at 150 m (EP150) as a fraction of primary production (PP); X-axis: EPx/EP150 = POC flux at defined depths (EPx; here 400 and 800 m) as a fraction of POC flux at 150 m (EP150). The green cross (Fig.5a) is for station A3-1 (KEOPS-2). Since no PP data is available for that station, the EP/PP value has been arbitrarily set to 0. Isolines represent the modeled 1, 5, 10, 20 and 30% of PP export to depths >at 400 or 800 m, and represent export efficiency.

Figure 8: Temporal evolution of particulate biogenic Ba (Ba_{xs}; pM) in the upper 2000 m water column in the Polar Front meander. Graph constructed using Ocean Data View (Schlitzer, 2002; Ocean Data View; http://www.awi-bremerhaven.de/GEO/ODV).

Table captions

Table 1: Station locations, CTD cast number and bottom depth during KEOPS 2. Depth-weighted average values (DWAv) of mesopelagic Ba_{xs} (pM) and Ba_{xs} based mesopelagic POC remineralization (MR; mgC m^{-2} d^{-1}) integrated between 150-400 and 150-800 m depths. See text for further information on calculation.

Table 2: Comparison of mesopelagic POC remineralization (MR) with primary production (PP) and export production (EP). All fluxes in mg C m^{-2} d^{-1}. r-ratio is the ratio of MR over EP. EP/PP is the export efficiency. The C transfer efficiency at 400 and 800 m (T400, T800) is the fraction of C export (EP) at 150 m exiting through the 400 m (T400) or the 800 m (T800) horizons. See text for further information on calculation.

Appendix A: Excess particulate biogenic Ba (Ba_{xs}; pM) and particulate Al (nM) during KEOPS 2.

References

Armand, L.K., Crosta, X., Quéguiner, B., Mosseri, J., Garcia, N. : Diatoms preserved in surface sediments of the northeastern Kerguelen Plateau, Deep- Sea Res. Pt. II, 55, 677–692, 2008.

de Baar, H. J. W., Boyd, P. W., Coale, K. H., Landry, M.R., Tsud, A., Assmy, P., Bakker, D.C.E, Bozec, Y., Barber, R.T., Brzezinski, M.A., Buesseler, K.O., Boyé, M., Croot, P.L., Gervais, F., Gorbunov, Y., Harrison, P.J., Hiscock, W.T., Laan, P., Lancelot, C., Law, C.S., Levasseur, M., Marchetti, A., Millero, F.J., Nishika, J., Nojiri, Y., van Oijen, T., Riebesell, U., Rijkenberg, M.J.A., Saito, H., Takeda, S., Timmermans, K.R., Veldhuis, J.W., Waite, A.M., Wong, C.S.: Synthesis of iron fertilization experiments: From the iron age in the age of enlightenment, J. Geophys. Res., 110, C09S16, doi:10.1029/2004JC002601, 2005.

Blain, S., Tréguer, P., Belviso, S., Bucciarelli, E., Denis, M., Desabre, S., Fiala, M., Martin Jézéquel, V., Le Fèvre, J., Mayzaud, P., Marty, J.- C., and Razouls, S.: A biogeochemical study of the island mass effect in the context of the iron hypothesis: Kerguelen Islands, Southern Ocean, Deep-Sea Res. Pt. I, 48, 163-187, 2001.

Blain, S., Queguiner, B., Armand, L., Belviso, S., Bombled, B., Bopp, L., Bowie, A., Brunet, C., Brussaard, C., Carlotti, F., Christaki, U., Corbiere, A., Durand, I., Ebersbach, F., Fuda, J. -L., Garcia, N., Gerringa, L., Griffiths, B., Guigue, C., Guillerm, C., Jacquet, S., Jeandel, C., Laan, P., Lefevre, D., Lo Monaco, C., Malits, A., Mosseri, J., Obernosterer, I., Park, Y. -H., Picheral, M., Pondaven, P., Remenyi, T., Sandroni, V., Sarthou, G., Savoye, N., Scouarnec, L., Souhaut, M., Thuiller, D., Timmermans, K., Trull, T., Uitz, J., van Beek, P., Veldhuis, M., Vincent, D., Viollier, E., Vong, L., and Wagener, T.: Effect of natural iron fertilization on carbon sequestration in the Southern Ocean, Nature, 446, 1070-1074, 2007.

Blain, S., Quéguiner, B., and Trull, T.: The natural iron fertilization experiment keops (kerguelen ocean and plateau compared study): An overview, Deep-Sea Res. Pt. II, 55, 559–565, 2008.

Boyd, P. W., Bakker, D. C. E., Chandler, C.: A new database to explore the findings from large-scale ocean iron enrichments experiments, Oceanography, 25, 64–71, doi:10.5670/oceanog.2012.104, 2012.

Boyd, P. W., Law, C. S., Wong, C. S., Nojiri, Y., Tsuda, A., Levasseur, M., Takeda, S., Rivkin, R., Harrison, P. J., Strzepek, R., Gower, J., McKay, R. M., Abraham, E., Arychuk, M., Barwell-Clarke, J., Crawford, W., Crawford, D., Hale, M., Harada, K., Johnson, K., Kiyosawa, H., Kudo, I., Marchetti, A., Miller, W., Needoba, J., Nishioka, J., Ogawa, H., Page, J., Robert, M., Saito, H., Sastri, A., Sherry, N., Soutar, T., Sutherland, N., Taira, Y., Whitney, F., Wong, S. K. E., and Yoshimura, T.: The decline and fate of an iron-induced subarctic phytoplankton bloom, Nature, 428, 549–553, 2004.

Boyd, P. W., Watson, A. J., Law, C. S., Abraham, E. R., Trull, T., Murdoch, R., Bakker, D. C. E., Bowie, A. R., Buesseler, K. O., Chang, H., Charette, M., Croot, P., Downing, K., Frew, R., Gall, M., Hadfield, M., Hall, J., Harvey, M., Jameson, G., LaRoche, J., Liddicoat, M., Ling, R., Maldonado, M. T., McKay, R. M., Nobber, S., Pickmere, S., Pridmore, R., Rintoul, S., Safi, K., Sutton, P., Strzepek, R., Tanneberger, K., Turner, S., Waite, A., and Zeldis, J.: Phytoplankton bloom upon mesoscale iron fertilization of polar Southern Ocean water, Nature, 407, 695–702, 2000.

Bowie, A. R., van der Merwe, P., Quéroué, F., Trull, T., Fourquez, M., Planchon, F., Sarthou, G., Chever, F., Townsend, A. T., Obernosterer, I., Sallée, J.-B., and Blain, S.: Iron budgets for three distinct biogeochemical sites around the Kerguelen archipelago (Southern Ocean) during the natural fertilisation experiment KEOPS-2, Biogeosciences Discuss., 11, 17861-17923, doi:10.5194/bgd-11-17861-2014, 2014.

Broecker, W. S., Takahashi, T., Takahashi, T.: Sources and flow patterns of deep-ocean waters as deduced from potential temperature, salinity and initial phosphate concentration, J. Geophys. Res., 90, 6925-6939, 1985.

Buesseler, K. O., Andrews, J.E., Pike, S.M., Charette, M.A.: The effect of iron fertilization on carbon sequestration in the Southern Ocean, Science, 304, 414– 417, 2004.

Buesseler, K.O., Andrews, J.E., Pike, S.M., Charette, M.A., Goldson, L.E., Brzezinski, M.A., Lance, V.P.: Particle export during the Southern Ocean Iron Experiment (SOFeX), Limnol. Oceanogr., 50 (1), 311– 327, 2005.

Buesseler, K.O., Antia, A.N., Chen, M., Fowler, S.W., Gardner, W.D., Gustaffson, Ö., Harada, K., Michaels, A.F., Rutgers van der Loeff, M., Sarin, M., Steinberg, D.K., Trull, T.: An assessment of the use of sediment traps for estimating upper ocean particle fluxes. Journal of Marine Research, 65(3): 345-416, 2007a.

Buesseler, K.O., Lamborg, C.H., Boyd, P.W., Lam, P.J., Trull, T.W., Bidigare, R.R., Bishop, J. K. B., K.L., Casciotti, Dehairs, F. , Elskens, M. , Honda, M. , Karl, D. M., Siegel, D. A., Silver, M. W., Steinberg, D.K. , Valdes, J., Van Mooy, B. , Wilson, S. : Revisiting carbon flux through the ocean's twilight zone, Science, 316, 567–569, 2007b.

Buesseler, K.O., and Boyd, P.W.: Shedding light on processes that control particle export and flux attenuation in the twilight zone. Limnol. Oceanogr., 54 (4), 1210-1232, 2009.

Cardinal, D., Dehairs, F., Cattaldo, T., and André, L.: Constraints on export and advection in the Subantarctic and Polar Front Zones, south of Australia from the geochemistry of suspended particles, J. Geophys. Res.-Oceans, 106, 31637-31656, doi : 10,1029/2000JC000251, 2001

Cardinal, D., Savoye, N., Trull., T.W., André, L., Kopczynska, E., Dehairs, F., 2005. Particulate Ba distributions and fluxes suggest latitudinal variations of carbon mineralization in the Southern ocean, Deep-Sea Res. Pt. I, 52, 355-370, 2005.

Carlotti, F., Jouandet, M.-P., Nowaczyk, A., Harmelin-Vivien, M., Lefèvre, D., Guillou, G., Zhu, Y., Zhou, M. : Mesozooplankton structure and functioning during the onset of the Kerguelen Bloom during Keops2 survey, this issue, in prep.

Cavagna, A. J., Fripiat, F., Elskens, M., Dehairs, F., Mangion, P., Chirurgien, L., Closset, I., Lasbleiz, M., Flores–Leiva, L., Cardinal, D., Leblanc, K., Fernandez, C., Lefèvre, D., Oriol, L., Blain, S., and Quéguiner, B.: Biological productivity regime and associated N cycling in the vicinity of Kerguelen Island area, Southern Ocean, Biogeosciences Discuss., 11, 18073-18104, doi:10.5194/bgd-11-18073-2014, 2014.

Closset, I., Lasbleiz, M., Leblanc, K., Quéguiner, B., Cavagna, A.-J., Elskens, M., Navez, J., and Cardinal, D.: Seasonal evo- lution of net and regenerated silica production around a natu- ral Fe-fertilized area in the Southern Ocean estimated from Si isotopic approaches, Biogeosciences, 11, 5827-5846, doi: 10.5194/bg-11-5827-2014, 2014.

Christaki, U., Obernosterer, I., VanWambeke, F., Veldhuis, M., Garcia, N., and Catala, P.: Microbial food web structure in a naturally iron fertilized area in the southern ocean (Kerguelen plateau), Deep-Sea Res. Pt. II, 55, 706–719, 2008.

Christaki, U., Lefèvre, D., Geoges, C., Colombet, J., catala, P., Courties, C., Sime-Ngando, T., Blain, S., and Obernosterer, I.: Microbial food web dynamics during spring phytoplankton blooms in the naturally iron-fertilized Kerguelen area (Southern Ocean), Biogeosciences, 11, 6739-3753, doi:10.5194/bg-11-6739-2014, 2014.

Dehairs, F., Chesselet, R., Jedwab, J.: Discrete suspended particles of barite and the barium cycle in the open ocean, Earth Planet. Sc. Lett., 49, 40-42, 1980.

Dehairs, F., Baeyens, W., Goeyens, L.: Accumulation of suspended barite at mesopelagic depths and export production in the Southern Ocean, Science, 258, 1332–1335, 1992.

Dehairs, F., Shopova, D., Ober, S., Veth, C., Goeyens, L.: Particulate barium stocks and oxygen consumption in the Southern Ocean mesopelagic water column during spring and early summer: Relationship with export production, Deep-Sea Res. Pt II, 44, 497-516, 1997.

Dehairs, F., Jacquet, S.H.M., Savoye, N., van Mooy, B., Buesseler, K., Bishop, J., Lamborg, C., Elskens, M., Baeyens, W., Casciotti K., Monnin , C.: Barium in twilight zone suspended matter as proxy for organic carbon mineralization: results for the North Pacific, Deep-Sea Res. Pt. II, 55, 1673-1683, 2008.

Dehairs, F., Fripiat, F., Cavagna, A.-J., Trull, T. W., Fernandez, C., Davies, D., Roukaerts, A., Fonseca Batista, D., Planchon, F., and Elskens, M.: Nitrogen cycling in the Southern Ocean Kerguelen Plateau area: evidence for significant surface nitrification from nitrate isotopic compositions, Biogeosciences Discuss., 11, 13905-13955, doi:10.5194/bgd-11-13905-2014, 2014.

D'ovidio, F., Della Penna, A., Trull, T.W., Nencioli, F., Pujol, I., Rio, M.H., Park, Y.H., Cotté, C., Zhou, M., Blain, S.: The biogeochemical structuring role of horizontal stirring: Lagrangian perspectives on iron delivery downstream of the Kerguelen plateau, in prep., this issue.

Dymond, J.R., Suess, E., Lyle, M.: Barium in deep-sea sediment: a geochemical proxy for paleoproductivity, Paleoceanography, 7, 163–181, 1992.

Ellison, Eurachem/CITAC Guide CG4, Quantifying Uncertainty in Analytical Measurement. Eds. S.L.R. Ellison, M. Rosslein and A. Williams. Second edition ISBN 0948926 15 5, Pp 120, 2000.

François, R., Honjo, S., Krishfield, R., and Manganini, S.: Factors controlling the flux of organic carbon to the bathypelagic zone of the ocean, Global Biogeochem. Cy., 16(4), 1087 doi:10.1029/2001GB001722, 2002.

Gervais, F., Riebesell, U., Gorbunov, M. Y.: Changes in primary productivity and chlorophyll a in response to iron fertilization in the southern Polar Frontal Zone, Limnol. Oceanogr., 47, 1324–1335, 2002.

Henson, S. A., et al. (2011), A reduced estimate of the strength of the ocean's biological carbon pump, Geophys. Res. Lett., 38(4), L04606.

Hoffmann, L., Peeken, I., Lochte, K., Assmy, P., Veldhuis, M.: Different reactions of Southern Ocean phytoplankton size classes to iron fertilization, Limnol. Oceanogr, 51, 1217–1229, 2006.

Jacquet, S.H.M., Dehairs, F., Cardinal, D., Navez, J., Delille, B.: Barium distribution across the Southern Ocean Frontal system in the Crozet-Kerguelen Basin, Mar. Chem., 95(3-4), 149-162, 2005.

Jacquet, S.H.M., Dehairs, F., Elskens, M., Savoye, N., Cardinal, D.: Barium cycling along WOCE SR3 line in the Southern Ocean, Mar. Chem., 106, 33-45, 2007.

Jacquet, S.H.M., Dehairs, F., Savoye, N., Obernosterer, I., Christaki, U., Monnin, C., Cardinal, D.: Mesopelagic organic carbon mineralization in the Kerguelen Plateau region tracked by biogenic particulate Ba, Deep-Sea Res. Pt. II, 55 (5-7), 868-879, 2008a.

Jacquet, S.H.M., Savoye, N Dehairs, F., Strass, V., Cardinal, D.: Mesopelagic carbon mineralization during the European Iron Fertilization Experiment (EIFEX), Glob. Biogeochem. Cy., 22, GB1023, doi:10.1029/2006GB002902, 2008b.

Jacquet, S.H.M., Dehairs, F., Becquevort, S., Dumont, I., Cavagna, A., Cardinal, D.: Twilight zone organic carbon remineralization in the PFZ and SAZ south of Tasmania (Southern Ocean), Deep-Sea Res. Pt. II, 58 (22-21), 2222-2234 doi:10.1016/j.dsr2.2011.05.029, 2011a.

Jacquet, S.H.M., Lam, P., Trull ,T., Dehairs, F.: Carbon export production in the Polar front zone and Subantarctic Zone south of Tasmania, Deep-Sea

Res. Pt. II, 58 (21-22), 2277-2292 doi:10.1016/j.dsr2.2011.05.035, 2011b.

Jouandet, M.P., and others: Particles distribution in contrasted area of the iron fertilized region around Kerguenlen Islans, in prep., this issue.

Lam, P. J., and Bishop, J. K. B.: High biomass, low export regimes in the Southern Ocean, Deep-Sea Research II, 54, 601-638, 2007.

Lampitt, R. S., Achterberg, E.P., Anderson, T.R., Hughes, J.A., Iglesisas-Rodriguez, M.D., Kelly-Gerreyn, B.A., Lucas, M., Popova, E.E., Sanders, R., Shepherd, J.G., Smythe-Wright, D., Yool, A. : Ocean fertilization: A potential means of geoengineering?, Philos. Trans. R. Soc. A, 366, 3919–3945, doi:10.1098/rsta.2008.0139, 2008.

Lampitt, R. S., Antia, A.N.: Particle flux in deep seas: regional characteristics and temporal variability, Deep-Sea Res. Pt I, 44, 1377-1403, 1997.

Lasbleiz, M., Leblanc, K., Blain, S., Ras, J., Cornet-Barthaux, V., Hélias Nunige, S., and Quéguiner, B.: Pigments, elemental composition (C, N, P, and Si), and stoichiometry of particulate matter in the naturally iron fertilized region of Kerguelen in the Southern Ocean, Biogeosciences, 11, 5931–5955, doi::10.5194/bg-11- 5931-2014, 2014.

Laurenceau-Cornec, E. C., Trull, T. W., Davies, D. M., Bray, S. G., Doran, J., Planchon, F., Carlotti, F., Jouandet, M.-P., Cavagna, A.-J., Waite, A. M., and Blain, S.: The relative importance of phytoplankton aggregates and zooplankton fecal pellets to carbon export: insights from free-drifting sediment trap deployments in naturally iron-fertilised waters near the Kerguelen plateau, Biogeosciences Discuss., 11, 13623-13673, doi:10.5194/bgd-11-13623-2014, 2014.

Laws, E. A., et al. (2000), Temperature effects on export production the ocean, Global Biogeochem. Cycles, 14(4), 1231–1246.

Lefèvre, D., Guigue, C., Obernosterer, I.: The metabolic balance at two contrasting sites in the Southern Ocean: the iron-fertilized Kerguelen area and HNLC waters, Deep-Sea Res. Pt. II, 55, 766–776, doi:10.1016/j.dsr2.2007.12.006, 2008.

Le Moigne, F. A. C., Moore, C. M., Sanders, R. J., Villa-Alfageme, M., Steigenberger, S., and Achterberg, E. P.: Sequestration efficiency in the iron-limited North Atlantic: Implications for iron supply mode to fertilized blooms, Geophys. Res. Lett., 41, doi:10.1002/2014GL060308, 2014.

Longhurst, A.R., Bedo, A.W., Harrison, W.G., Head, E.J.H., Sameoto, D.D. : Vertical flux of respiratory carbon by oceanic diel migrant biota, Deep-Sea Res Pt, 37 (4), 685–694, 1990.

Maiti, K., Charette, M., Buesseler, K., and Kahru, M.: An inverse relationship between production and export efficiency in the Southern Ocean, Geophys. Res. Lett., 40, 2013.

Martin, J.H., Knauer, G.A., Karl, D.M., Broenkow, W.W.: VERTEX: carbon cycling in the NE Pacific, Deep-Sea Res., 34, 267–285, 1987.

Monnin, C., Jeandel, C., Cattaldo, T., Dehairs, F.: The marine barite saturation state of the world's oceans, Mar. Chem., 65(3-4), 253-261, 1999.

Morris, P.J, and Charette, M.A.: A synthesis of upper oceancarbon and dissolved iron budgets for Southern Ocean natural iron fertilization studies (2013), Deep-Sea Res., 90, 147-157, 2013.

Passow, U., Carlson, C. A. : The biological pump in a high CO2 world, Mar. Ecol. Prog. Ser., 470, 249–271, doi:10.3354/meps09985, 2012.

Porris, P.J., Sanders, R., Turnewithsch, R., Thomalla, S., 234^{Th}-derived particulate organic carbon export from an island-induced phytoplankton blomm in the Southern Ocean,Deep-Sea Res. Pt.II, 24, 2208-2232, 2007

Mosseri, J., Quéguiner, B., Armand, L. K., and Cornet-Barthaux, V.: Impact of iron on silicon utilization by diatoms in the Southern Ocean: a case study of Si/ N cycle decoupling in a naturally iron-enriched area, Deep-Sea Res. Pt. II, 55, 801-819, doi :10,1016/j.dsr2,2007,12,003, 2008.

Park, Y. H., Durand, I., Kestenare, E., Rougier, G., Zhou, M., d'Ovidio, F., Cotté, C., and Lee J. H.: Polar front around the Kerguelen islands: An up-to-date determination and associated circulation of surface/subsurface water. J. Geophys. Res. Oceans, 119, i10.1002/2014JC010061, 2014.

Park, Y.-H., Roquet, F., Durand, I., and Fuda, J.-L.: Large-scale circulation over and around the Northern Kerguelen Plateau, Deep-Sea Res. Pt. II, 55, 566–581, doi:10.1016/j.dsr2.2007.12.030, 2008.

Planchon, F., Cavagna A.J., Cardinal, D., André, L., Dehairs, F. Late summer particulate organic carbon export and twilight zone remineralisation in the Atlantic sector of the Southern Ocean, Biogeosciences, 10, 803–820, doi:10.5194/bg-10-803-2013, 2013.

Planchon, F., Ballas, D., Cavagna A. J., Van Der Merwe, P., Bowie, A., Trull, T., Laurenceau, E., Davis, D., and Dehairs, F.: Carbon export in the naturally iron fertilized Kerguelen area of the Southern Ocean using 234Th-based approach, in prep., 2014.

Pollard, R. T., Salter, I., Sanders, R. J., Lucas, M. I., Moore, C. M., Mills, R. A., Statham, P. J., Allen, J. T., Baker, A. R., Bakker, D. C. E., Charette, M. A., Fielding, S., Fones, G. R., French, M., Hickman, A. E., Holland, R. J., Hughes, J. A., Jickells, T. D., Lampitt, R. S., Morris, P. J., Nedelec, F. H., Nielsdottir, M., Planquette, H., Popova, E. E., Poulton, A. J., Read, J. F., Seeyave, S., Smith, T., Stinchcombe, M., Taylor, S., Thomalla, S., Venables, H. J., Williamson, R., and Zubkov, M. V.: Southern Ocean deep-water carbon export enhanced by natural iron fertilization, Nature, 457, 577-U581, Doi 10.1038/Nature07716, 2009.

Quéroué, F., Sarthou, G., Planquette, H. F., Bucciarelli, E., Chever, F., van der Merwe, P., Lannuzel, D., Townsend, A. T., Cheize, M., Blain, S., d'Ovidio, F., and Bowie, A. R.: High variability of dissolved iron concentrations in the vicinity of Kerguelen Island (Southern Ocean), Biogeosciences Discuss., 12, 231-270, doi:10.5194/bgd-12-231-2015, 2015.

Rembauville, M., Blain, S., Armand, L., Quéguiner, B., and Salter, I.: Export fluxes in a naturally fertilized area of the Southern Ocean, the Kerguelen Plateau: ecological vectors of carbon and biogenic silica to depth (Part 2), Biogeosciences Discuss., 11, 17089-17150, doi:10.5194/bgd-11-17089-2014, 2014.

Robinson, J., Popova, E. E., Yool, A., Srokosz, M. A., Lampitt, R. S., and Blundell, J. R.: How deep is deep enough? Ocean iron fertilization and carbon sequestration in the Southern Ocean, Geophys. Res. Lett., 41, 2489-2495, 2014.

Salter, I., Lampitt, R.S., Sanders, R., Poulton, A., Kemp, A.E.S., Boorman, B., Saw, K., Pearce, R.: Estimating carbon, silica and diatom export from a naturally fertilised phytoplankton bloom in the Southern Ocean using PELAGRA: a novel drifting sediment trap, Deep-Sea Res. Pt. II, 54, 2233–2259, 2007.

Sarmiento, J.L., Slater, R.D., Fasham, M.J.R., Ducklow, H.W., Toggweiler, J.R.: A seasonal three-dimensional ecosystem model of nitrogen cycling in the North Atlantic photic zone, Global Biogeochem. Cy., 7, 417–450, 1993.

Savoye, N., Trull, T., Jacquet, S.H.M., Navez, J., Dehairs, F.: ^{234}Th-derived export fluxes during a natural iron fertilization experiment (KEOPS), Deep-Sea Res. Pt. II, 55 (5-7), 841-855, 2008.

Schlitzer, R., Ocean Data View, http://www.awi-bremerhaven.de/GEO/ODV, 2002.

Schneider, B., Bopp, L., Gehlen, M.: Assessing the sensitivity of modeled airsea CO2 exchange to the remineralization depth of particulate organic and inorganic carbon, Global Biogeochem. Cy., 22, GB3021, doi:10.1029/2007GB003100, 2008.

Shopova, D., Dehairs, F., Baeyens, W.: A simple model of biogeochemical element distribution in the oceanic water column, J. Mar. Sy., 6, 331–344, 1995.

Smetacek, V., Klass, C., Strass, V.H., Assmy, P., %ontresor, M., Cisewki, B., Savoye, N., Webb, A., d'Ovidio, F., Arrieta, J.M., Bathmann, U., Bellerby, R., Mine Berg, G., Croot, P., Gonzalez, S., Jenjes, J., Herndl, G.J., Hoffmann, L.J., Leach, H., Losh, M., Mills, M.M., Neill, C., Peeken, I., Rottgers, R., Sachs, O., Sauter, E., Schmidt, M.M., Schwarz, J., Terbruggen, A., Wolf-Gladrow, D. : Deep carbon export from a Southern Ocean iron-fertilized diatom bloom, Nature, 487, 313–319, doi:10.1038/nature11229, 2012.

Sternberg, E., Jeandel, C., Miquel, J.-C., Gasser, B., Souhaut, M., Arraes-Mescoff, R., Francois R. : Particulate barium fluxes and export production in the northwestern Mediterranean. Mar. Chem. 105, 281–295, 2007.

Sternberg, E., Jeandel, C., Robin, E., Souhaut, M.: Seasonal cycle of suspended barite in the Mediterranean Sea, Geochimica et Cosmochimica Acta, 72, 4020-4034, 2008a.

Sternberg, E., Tang, D., Ho, T_Y., Jeandel, C., Morel, M.M..: Barium uptake and adsorption in diatoms, Geochimica et Cosmochimica Acta, 69, 11, 2745-2752, 2008b.

Strass, V., Cisewski, B., Gonzales, S., Leach, H., Loquay, K.-D., Prandke, H., Rohr, H., Thomas, M.: The physical setting of the European Iron Fertilization Experiment 'EIFEX' in the Southern Ocean, Reports on Polar and Marine Research, 500, 15–49, 2005.

Stroobants, N., Dehairs, F., Goeyens, L., Vanderheijden, N., Van Grieken, R.: Barite formation in the Southern Ocean water column, Mar. Chem., 35, 411-422, 1991.

Taylor, S.R., McLennan, S.M.: The continental crust: its composition and evolution, Blackwell Scientific Publications, 312pp, 1985.

van der Merwe, P., Bowie, A. R., Quéroué, F., Armand, L., Blain, S., Chever, F., Davies, D., Dehairs, F., Planchon, F., Sarthou, G., Townsend, A. T., and Trull, T.: Sourcing the iron in the naturally-fertilised bloom around the Kerguelen Plateau: particulate trace metal dynamics, Biogeosciences Discuss., 11, 13389-13432, doi:10.5194/bgd-11-13389-2014, 2014.

Venchiarutti, C., Jeandel, C., Roy-Barman, M.: Particle dynamics study in the wake of Kerguelen Island using thorium isotopes, Deep-Sea Res. Pt. I, 55, 1343–1363, 2008.

Williams, P.J., Jenkinson, N.W. : A transportable microprocessor-controlled precise Winkler titration suitable for field station and shipboard use. Limnol. Oceanogr. 27, 576-585, 1982.

Zhou, M., Zhu, Y., Dorland, R.D., Measures, C.I.: Dynamics of the current system in the southern Drake Passage, Deep-Sea Res. Pt I, 57, 1039–1048, 2010.

Zhou, M., Zhu, Y., Measures, C.I., Hatta, M., Charette, M.A., Gille, S.T., Frants, M., Jiang, M., Mitchell, B.G.: Winter mesoscale circulation on the shelf slope region of the southern Drake Passage, Deep-Sea Res. Pt II, 90, 4–14, 2013.

Zhou, M., and others: Estimates of particle settling and scavenging using LISST-LOPC in Kergueln Plateau regions during the 2011 austral spring KEOPS II cruise, in prep., this issue.

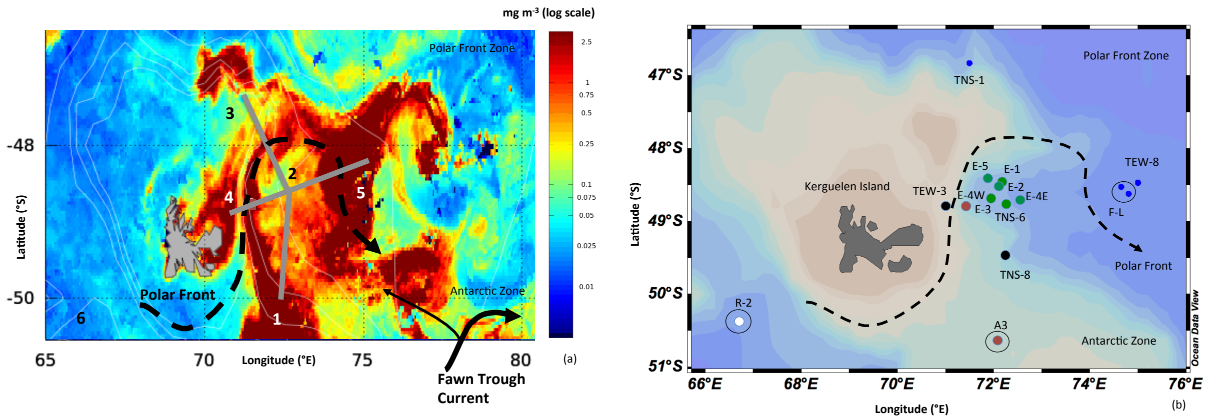

mg m⁻³ (log scale)
2.5
1
0.75
0.5
0.25
0.1
0.075
0.05
0.025
0.01
Polar Front Zone
3
2
4
5
-48
Latitude (°S)
-50
Polar Front
6
1
Antarctic Zone
65
70
Longitude (°E)
75
80
(a)
Fawn Trough
Current
47°S
48°S
49°S
50°S
51°S
TNS-1
Polar Front Zone
Kerguelen Island
TEW-3
E-5
E-1
E-2
E-4W
E-4E
E-3
TNS-6
TEW-8
F-L
Polar Front
TNS-8
R-2
A3
Antarctic Zone
Latitude (°S)
66°E
68°E
70°E
72°E
74°E
76°E
Longitude (°E)
(b)
Ocean Data View

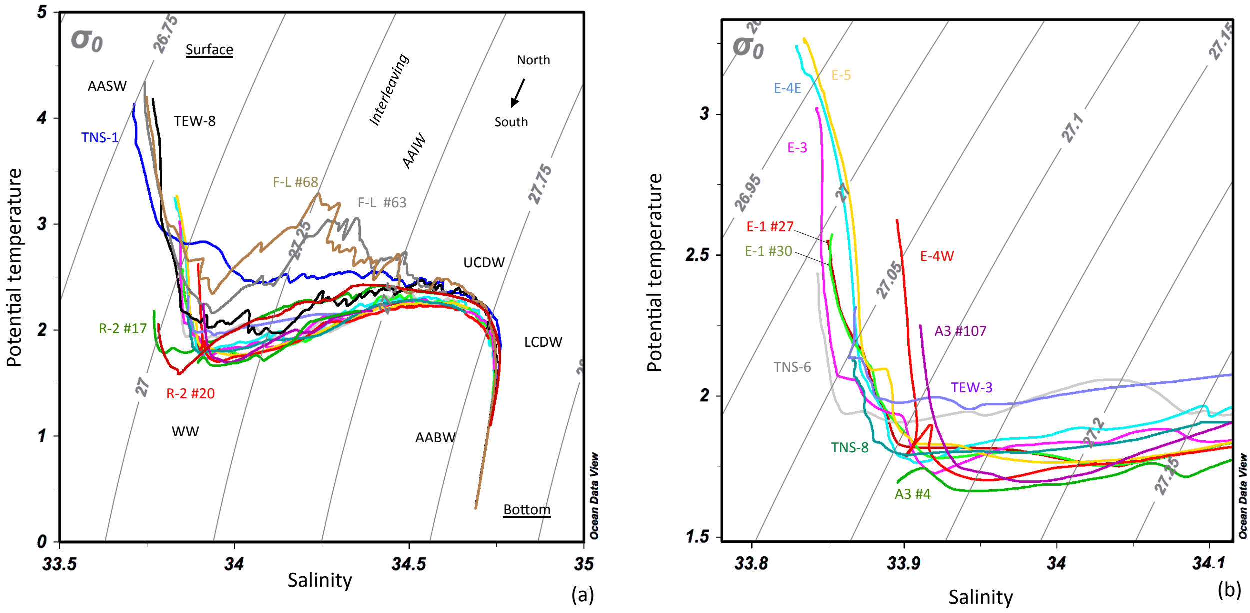

σ0
Surface
AASW
TNS-1
TEW-8
Interleaving
AAIW
North
South
F-L #68
F-L #63
UCDW
LCDW
R-2 #17
R-2 #20
WW
AABW
Bottom
26.75
27
27.25
27.75
Potential temperature
Salinity
Ocean Data View
(a)
σ0
E-4E
E-5
E-3
E-1 #27
E-1 #30
E-4W
A3 #107
TNS-6
TEW-3
TNS-8
A3 #4
26.95
27
27.05
27.1
27.15
27.2
27.25
Potential temperature
Salinity
Ocean Data View
(b)

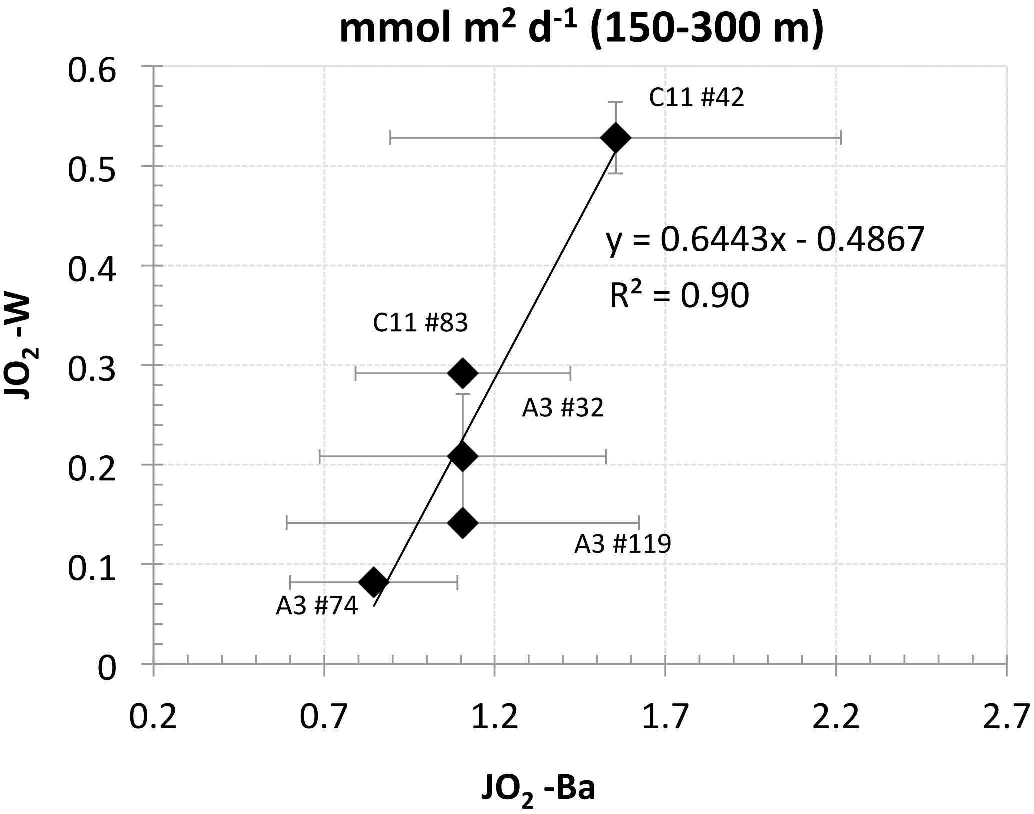

mmol m² d⁻¹ (150-300 m)
C11 #42
y = 0.6443x - 0.4867
R² = 0.90
C11 #83
A3 #32
A3 #119
A3 #74
JO2 -W
JO2 -Ba
0.6
0.5
0.4
0.3
0.2
0.1
0
0.2
0.7
1.2
1.7
2.2
2.7

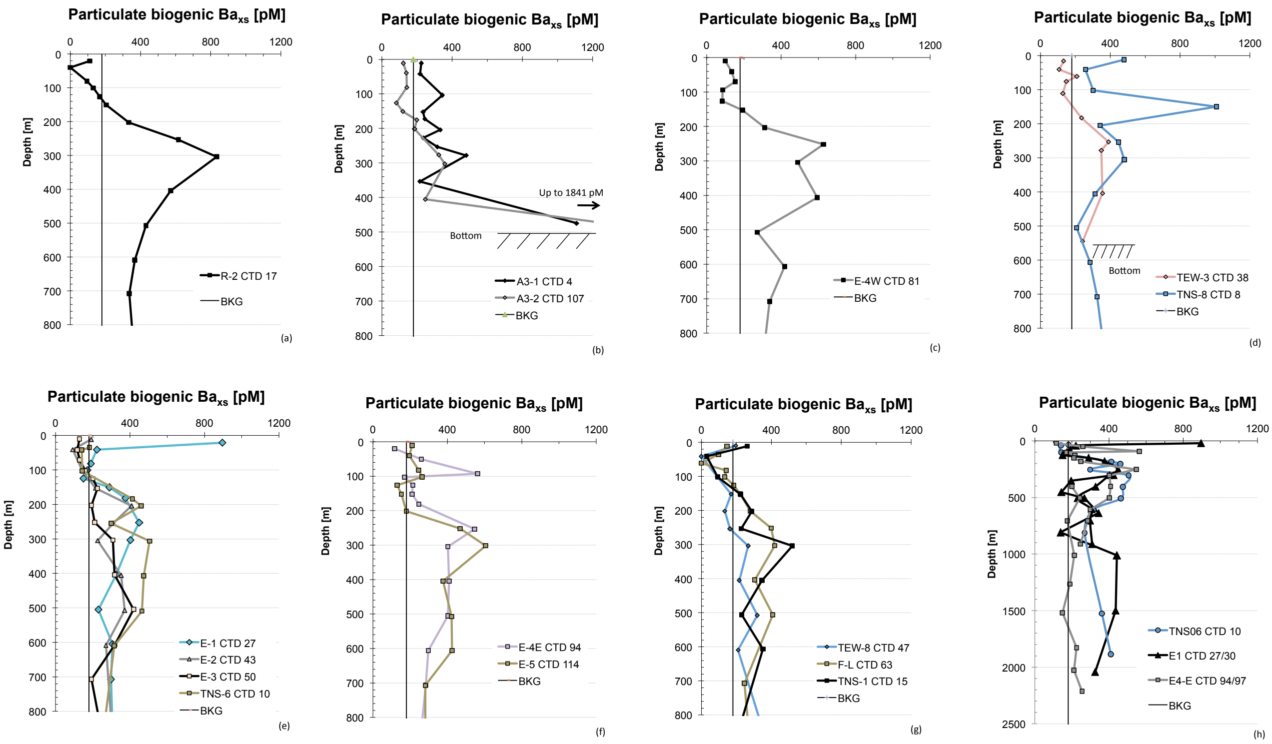

Particulate biogenic Ba$_{xs}$ [pM]
Depth [m]
R-2 CTD 17
BKG
(a)
A3-1 CTD 4
A3-2 CTD 107
BKG
Up to 1841 pM
Bottom
(b)
E-4W CTD 81
BKG
(c)
TEW-3 CTD 38
TNS-8 CTD 8
BKG
Bottom
(d)
E-1 CTD 27
E-2 CTD 43
E-3 CTD 50
TNS-6 CTD 10
BKG
(e)
E-4E CTD 94
E-5 CTD 114
BKG
(f)
TEW-8 CTD 47
F-L CTD 63
TNS-1 CTD 15
BKG
(g)
TNS06 CTD 10
E1 CTD 27/30
E4-E CTD 94/97
BKG
(h)

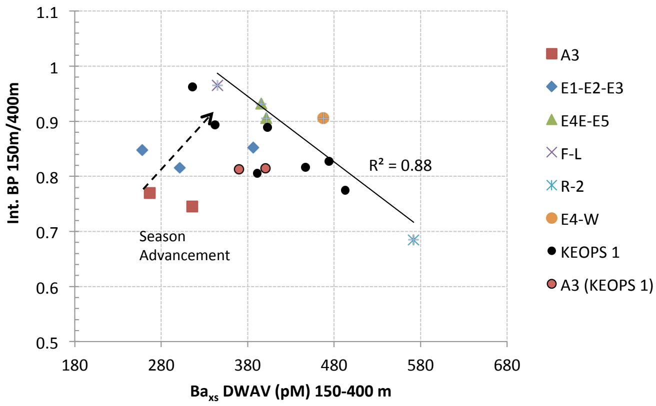

Int. BP 150m/400m
1.1
1
0.9
0.8
0.7
0.6
0.5
180
280
380
480
580
680
Ba$_{xs}$ DWAV (pM) 150-400 m
R^2 = 0.88
Season Advancement
A3
E1-E2-E3
E4E-E5
F-L
R-2
E4-W
KEOPS 1
A3 (KEOPS 1)

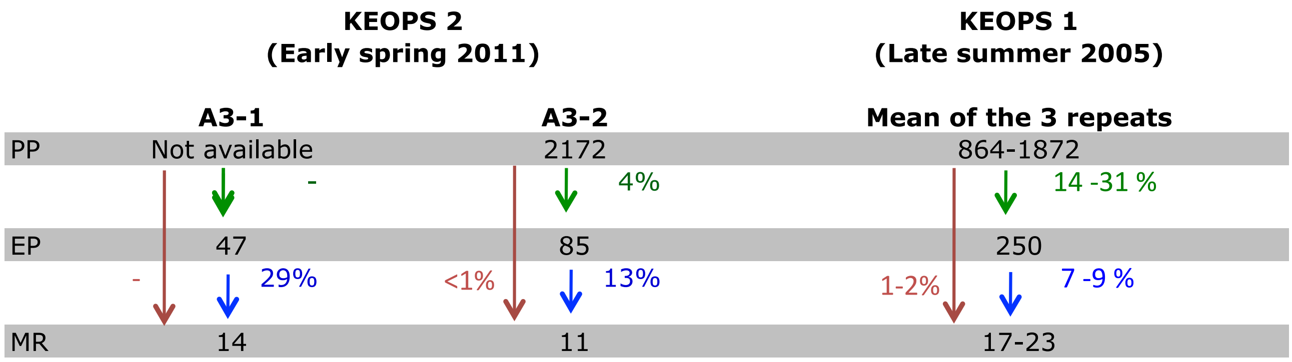

All fluxes in mgC m^{-2} d^{-1}
Blue values: r-ratio, mesopelagic remineralization efficiency (MR/EP)
Grenn values: EP/PP
Red values: MR/PP

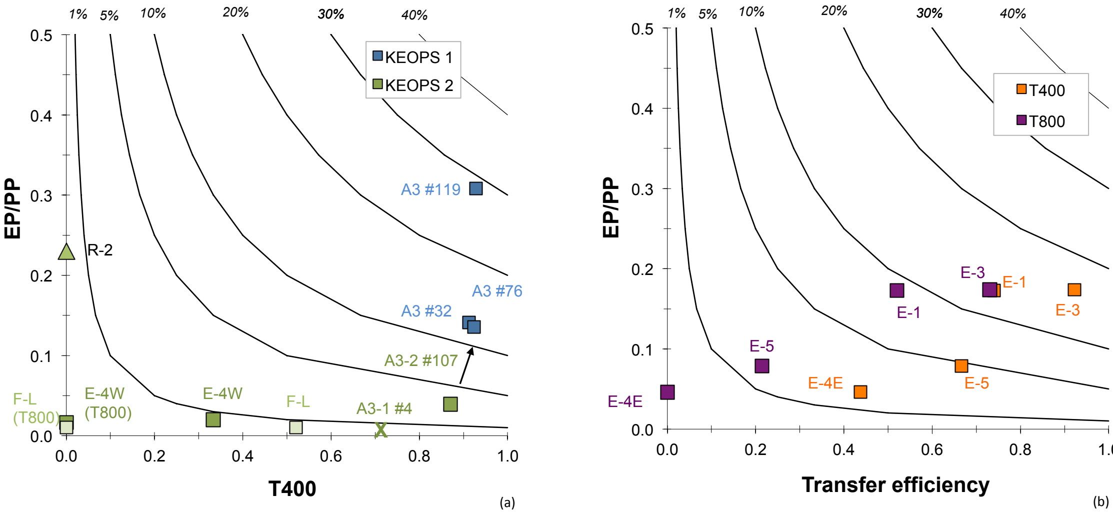

1%
5%
10%
20%
30%
40%
KEOPS 1
KEOPS 2
EP/PP
T400
A3 #119
R-2
A3 #76
A3 #32
A3-2 #107
F-L
(T800)
E-4W
(T800)
E-4W
F-L
A3-1 #4
(a)
T400
T800
Transfer efficiency
E-3
E-1
E-1
E-3
E-5
E-4E
E-5
E-4E
(b)

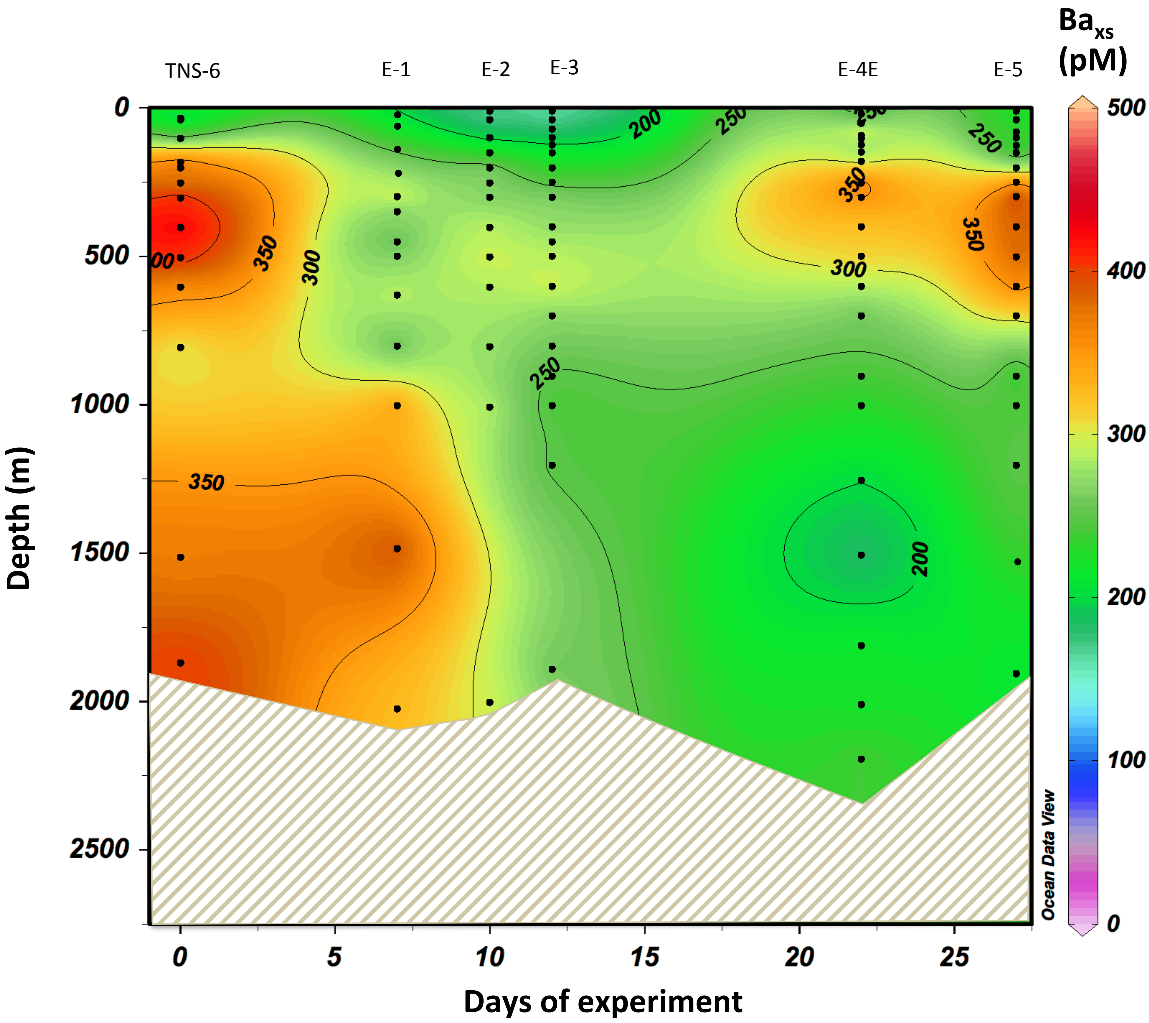

Ba$_{xs}$ (pM)
TNS-6
E-1
E-2
E-3
E-4E
E-5
Depth (m)
Days of experiment
Ocean Data View
0
500
1000
1500
2000
2500
0
5
10
15
20
25
100
200
300
400
500
200
250
300
350

Station	CTD cast #	Long (°E)	Lat (°S)	Date of sampling	Seafloor [m]	DWAv° Ba_{xs} [pM] 150- 400 m	DWAv Ba_{xs} [pM] 150- 800 m	MR°° 150- 400 m [mgC/m^2/d]	MR Stnd Uncertainty %	MR 150- 800 m [mgC/m^2/d]	MR Stnd Uncertainty %
Plateau											
A3-1	4*	72.080	50.629	20/10	530	316	/	14	4	/	/
A3-2	107*	72.056	50.624	16/11	527	267	/	11	5	/	/
TEW-3	38	71.018	48.799	31/10	560	324	/	28	8	/	/
Meander time series											
TNS-6	10	72.277	48.779	22/10	1885	427	389	31	7	69	17
E-1	27/30	72.187	48.458	29,30/10	2056	387	325	26	6	48	14
E-2	43	72.077	48.523	1/11	2003	301	309	15	5	42	13
E-3	50/55	71.967	48.702	03,04/11	1915	258	286	10	4	35	12
E-4E	94/97	72.563	48.715	13,14/11	2210	395	357	27	7	58	15
E-5	113/114	71.900	48.412	18/11	1920	402	380	28	7	66	17
Polar Front Zone											
TNS-1	15	71.501	46.833	23/10	2280	350	315	22	6	45	14
TEW-8	47	74.999	48.471	2/11	2786	199	240	2	4	20	11
F-L	63/68	74.659	48.532	06,07/11	2695	345	328	21	6	49	14
Polar Front											
E-4W	81/87	71.425	48.765	11,12/11	1384	468	411	36	8	76	18
Antarctic Zone											
R-2 (Reference site)	17/20	66.717	50.359	25,26/10	2300	572	456	50	10	91	20
TNS-8	8	72.240	49.463	21/10	1030	473	358	37	8	59	15

*Station A3 (CTD #4 and #107); integration up to 354 and 405 m
DWAV°= Depht weighted average value
MR°°= Mesopelagic C remineralization

Station	CTD	MLD [m]	Ez** [m]	PP° Ez [mgC/m^2/d]	EP°° 150 m [mgC/m2/d]	MR 150-400 m [mgC/m^2/d]	MR 150-800 m [mgC/m^2/d]	EP/PP	r-ratio 150-400 m	r-ratio 150-800 m	T400	T800
Plateau												
A3-1	4*	161	/	/	47	14	/	/	0.29	/	0.70	/
A3-2	107*	165	38	2172	85	11	/	0.04	0.13	/	0.87	/
Reference site												
R-2	17/20	111	92	132	30	50	91	0.23	1.65	3.02	0	0
Meander time series												
E-1	27/30	84	64	578	100	26	48	0.17	0.26	0.48	0.74	0.52
E-3	50/55	41	68	748	130	10	35	0.17	0.08	0.27	0.92	0.73
E-4E	94/97	77	34	1037	48	27	58	0.05	0.57	1.21	0.43	0.00
E-5	113/114	36	54	1064	84	28	66	0.08	0.33	0.78	0.67	0.22
Polar Front Zone												
F-L	63/68	21	29	3380	43	21	49	0.01	0.48	1.13	0.52	0
Polar Front												
E-4W	81/87	67	31	3287	54	36	76	0.02	0.67	1.41	0.33	0

*Station A3 (CTD4 and 107); MR integrated up to 354 and 405 m
**EZ euphotic layer (till 1% PAR level)
° PP data from Cavagna et al. (this issue)
°° EP data from PLanchon et al. (this issue)

Station A3

A3-1 CTD4

Niskin	Depth [m]	Ba_{xs} [pM]	Al [nM]
23	11	224	35
21	42	217	64
19	104	345	65
17	152	234	19
15	173	244	19
13	204	333	17
11	227	235	8
9	253	315	6
7	279	480	8
5	354	216	21
1	474	1108	155

A3-2 CTD 107

Niskin	Depth [m]	Ba_{xs} [pM]	Al [nM]
23	11	122	16
21	40	140	12
19	81	141	10
17	126	82	27
15	151	119	14
13	176	199	9
11	202	186	14
9	277	323	24
7	303	359	32
5	405	247	19
1	513	1842	186

Station RK2

R-2 CTD17

Niskin	Depth [m]	Ba_{xs} [pM]	Al [nM]
24	21	110	107
23	40	0	693
22	80	95	49
20	100	131	27
18	126	168	5
16	151	205	4
14	203	334	3
13	253	616	6
12	304	834	16
10	404	573	9
9	507	430	10
7	608	367	4
5	708	337	10
1	911	368	13

R-2 CTD 20

Niskin	Depth [m]	Ba_{xs} [pM]	Al [nM]
17	356	546	12
15	507	239	17
13	609	226	7
11	812	267	3
10	1011	189	2
8	1520	201	4
6	1832	184	2
1	2473	286	3

Station E

E-1 CTD 27

Niskin	Depth [m]	Ba_{xs} [pM]	Al [nM]
24	21	896	166
23	41	221	131
22	81	190	161
20	101	172	102
18	125	150	10
16	151	290	9
14	182	375	5
13	253	450	12
12	303	402	9
10	403	327	10
9	505	230	6
7	605	305	10
5	707	298	10
1	913	309	7

E-1 CTD 30

Niskin	Depth [m]	Ba_{xs} [pM]	Al [nM]
17	303	424	30
16	353	195	25
15	455	143	6
13	505	268	6
11	636	343	7
10	808	138	2
8	1011	442	4
6	1498	436	9
1	2042	326	7

E-2 CTD 43

Niskin	Depth [m]	Ba_{xs} [pM]	Al [nM]
23	11	192	43
21	41	93	152
18	102	143	17
16	153	215	57
14	204	408	9
12	254	311	6
10	305	227	4
8	406	353	5
7	507	371	9
6	609	271	10
5	813	297	14
4	1016	350	35
1	2020	302	11

E-3 CTD 50

Niskin	Depth [m]	Ba_{xs} [pM]	Al [nM]
24	11	129	45
23	42	117	93
22	71	130	28
20	102	160	22
18	125	201	11
16	153	225	18
14	203	193	3
13	252	210	2
12	304	309	6
10	404	316	7
9	505	419	64
7	606	320	14
5	707	193	12
1	912	265	5

Station E (continued)

E-3 CTD 55

Niskin	Depth [m]	Ba_{xs} [pM]	Al [nM]
17	404	185	5
16	455	272	5
15	505	176	6
13	605	378	5
11	810	258	3
10	910	172	2
8	1012	184	3
6	1214	228	6
1	1908	237	9

E-4W CTD 81

Niskin	Depth [m]	Ba_{xs} [pM]	Al [nM]
24	10	101	16
23	41	134	17
22	70	152	5
20	94	86	18
18	126	84	7
16	153	193	8
14	203	312	4
13	252	628	17
12	304	488	12
10	406	594	11
9	507	272	11
7	607	418	12
5	708	338	21
1	909	294	14

E-4W CTD 87

Niskin	Depth [m]	Ba_{xs} [pM]	Al [nM]
17	304	277	9
16	354	350	10
15	453	233	7
13	606	182	9
11	811	186	5
10	910	187	7
8	1011	268	61
6	1214	249	29
1	1384	250	30

E-4E CTD 94

Niskin	Depth [m]	Ba_{xs} [pM]	Al [nM]
24	20	116	32
23	51	260	11
22	93	563	223
20	103	170	5
18	126	215	9
16	152	210	6
14	181	247	7
13	253	547	4
12	305	403	78
10	404	408	26
9	505	403	26
7	606	298	13
5	706	285	8
1	912	245	65

Station E (continued)

E-4E CTD 97

Niskin	Depth [m]	Ba_{xs} [pM]	Al [nM]
21	404	199	2
18	505	242	3
13	706	175	1
8	1012	212	11
7	1265	189	2
6	1518	149	2
5	1827	225	43
4	2027	212	12
1	2212	254	9

E-5 CTD 113

Niskin	Depth [m]	Ba_{xs} [pM]	Al [nM]
10	911	111	3
8	1011	266	16
6	1214	256	15
1	1922	208	5

E-5 CTD 114

Niskin	Depth [m]	Ba_{xs} [pM]	Al [nM]
24	11	210	5
23	41	196	14
22	82	245	4
20	102	264	14
18	126	131	6
16	152	153	5
14	202	181	2
13	252	469	6
12	302	606	9
10	404	377	13
9	507	422	11
7	606	425	7
5	707	281	12
1	910	281	6

Transect West-East

TEW-3 CTD38

Niskin	Depth [m]	Ba_{xs} [pM]	Al [nM]
23	16	133	40
21	41	107	112
19	61	209	45
17	76	148	20
13	112	128	13
11	183	235	8
9	253	391	11
7	277	348	9
5	404	356	8
1	545	242	13

TEW-8 CTD 47

Niskin	Depth [m]	Ba_{xs} [pM]	Al [nM]
23	10	196	31
21	41	0	251
18	102	92	41
16	152	169	45
14	202	134	9
12	254	164	5
10	304	268	12
8	405	217	5
7	507	319	5
6	609	209	8
5	809	330	14
4	1011	334	22
1	2812	11179	826

Station F-L

F-L CTD 63

Niskin	Depth [m]	Ba_{xs} [pM]	Al [nM]
24	11	146	37
23	35	97	41
22	61	0	228
20	82	141	36
18	101	134	5
16	126	185	5
14	151	221	5
13	202	280	7
12	252	399	8
10	303	420	7
9	404	305	26
7	506	408	7
5	707	247	10
1	911	282	11

F-L CTD 68

Niskin	Depth [m]	Ba_{xs} [pM]	Al [nM]
17	405	264	6
16	456	233	9
15	506	339	12
13	607	265	3
11	910	718	7
10	1013	257	5
8	1215	316	8
6	1772	225	7
1	2741	2999	131

Transect North-South

TNS-1 CTD15

Niskin	Depth [m]	Ba_{xs} [pM]	Al [nM]
23	11	262	62
21	41	30	90
18	102	93	15
16	153	225	17
14	202	289	5
12	253	228	2
10	304	521	4
8	405	346	3
7	506	230	1
6	607	352	13
5	809	234	4
4	1520	127	6
1	2282	211	19

TNS-6 CTD 10

Niskin	Depth [m]	Ba_{xs} [pM]	Al [nM]
23	35	182	26
21	42	141	12
18	103	143	14
16	184	413	11
14	204	461	8
12	255	298	5
10	306	505	7
8	407	474	4
7	509	464	9
6	610	315	15
5	813	269	9
4	1526	362	13
1	1886	410	21

TNS-8 CTD8

Niskin	Depth [m]	Ba_{xs} [pM]	Al [nM]
23	12	478	45
21	41	258	53
18	102	303	32
16	150	1008	33
14	205	341	10
12	254	447	6
10	305	481	4
8	405	312	3
7	505	208	3
6	606	283	7
5	707	325	11
4	910	376	35
1	1000	294	28